Acta Geochim (2021) 40(4):557–574
https://doi.org/10.1007/s11631-021-00469-z

ORIGINAL ARTICLE

Zinc, copper, and strontium isotopic variability in the Baiyangping Cu–Pb–Zn–Ag polymetallic ore field, Lanping Basin, Southwest China

Caixia Feng[1] · Shen Liu[1] · Guoxiang Chi[2] · Xianwu Bi[3] · Ruizhong Hu[3] · Ian M. Coulson[2]

Received: 24 January 2021 / Revised: 4 March 2021 / Accepted: 22 March 2021 / Published online: 16 April 2021

Abstract The Baiyangping Cu–Ag polymetallic ore district is located in the northern part of the Lanping-Simao foreland fold belt, between the Jinshajiang-Ailaoshan and Lancangjiang faults, and the deposit can be divided into eastern and western ore zones. Based upon microscope observation of ore minerals and analysis of zinc, copper, and strontium isotope composition, we conclude that: (1) the zinc isotopic compositions of sphalerite from the eastern and western ore belt of the Baiyangping polymetallic ore deposits are enriched in both the heavy (− 0.09‰ to + 0.15‰) and light (− 0.19‰ to − 0.01‰) zinc isotopes. Rayleigh fractionation is likely the additional factor controlling the observed temporal and spatial variations in zinc isotopes in the two studied ore zones. The zinc isotopic composition in the Baiyangping polymetallic Pb–Zn deposits may have the same fractionation as that of magmatic-hydrothermal, VHMS, SEDEX, and MVT deposits, as demonstrated by geological and other geochemical evidence; (2) the range of δ^{65}Cu in massive tetrahedrite is from − 0.06‰ to + 0.12 ‰ that relates to the early stages of ore-formation, which are higher than that of venial chalcopyrite (from − 0.72‰ to − 0.07‰) formed at a late ore-forming stage in the western ore belt. Different ore-forming stages and alteration or leaching processes are likely the main factors controlling the observed variations in copper isotopes in the western ore zone; (3) the $^{87}Sr/^{86}Sr$ value of hydrothermal calcite in eastern (0.7080–0.7093) and western (0.7085–0.7113) ore belt suggested that mineralization of early calcite, with $^{87}Sr/^{86}Sr$ values much higher than in ancient Late Triassic seawater, may be related to recrystallization from a radiogenic Sr-rich or silicifying fluid, either from the strata that the ore-forming fluid flows through or from other fluids.

Keywords Zn–Cu–Sr isotopic variation · Cu–Pb–Zn–Ag poly-metallic ore deposit · Baiyangping · Lanping Basin

1 Introduction

Fe, Cu, Zn, Mo, Li, and Mg are examples of non-traditional metal stable isotopes (Zhu et al. 2001; Luck et al. 2003, 2005; Norman et al. 2004; Johnson et al. 2004a, b; Poitrasson et al. 2005; Weyer et al. 2005). Copper has two isotopes, ^{63}Cu, and ^{65}Cu, which in nature occur in the proportions: 69.17% and 30.83%, respectively (Shields et al. 1965). By contrast, zinc has five isotopes: ^{64}Zn, ^{66}Zn, ^{67}Zn, ^{68}Zn, and ^{70}Zn, naturally occurring in the following proportions: 48.63%, 27.92%, 4.10%, 18.75%, and 0.62%, respectively (Rosman 1972). With the advent of multi-collector-inductively coupled plasma-mass spectrometry (MC-ICP-MS) (Maréchal et al. 1999), it is now possible to study the isotope geochemistry of transition metals in natural systems (Thomas et al. 2005). Analytical protocols for Zn isotope analysis by MC-ICP-MS were developed in the late 1990s (Halliday et al. 1995; Maréchal et al. 1999) and early 2000s (Rehkämper et al. 2001; Maréchal and Albarède 2002; Archer and Vance 2004; Johnson et al.

✉ Caixia Feng
fengcaixia@nwu.edu.cn

[1] State Key Laboratory of Continental Dynamics, Department of Geology, Northwest University, 229 Taibai Road, Xi'an 710069, China

[2] Departments of Geology, University of Regina, 3737 Wascana Parkway, Regina, SK S4S 0A2, Canada

[3] Institute of Geochemistry, Chinese Academy of Sciences, 99 Lincheng Road, Guiyang 550002, China

2004a, b; Chapman 2006), and analyses based upon these protocols show substantial natural variations. Zinc isotope ratios are expressed in the δ notation ($\delta^{66}Zn = [(^{66}Zn/^{64}Zn)_{sample}/(^{66}Zn/^{64}Zn)_{standard} - 1] \times 1000$). In the case of copper, the isotopic ratio is commonly expressed in the following δ notation ($\delta^{65}Cu = [R_{sample}/R_{NIST976-} - 1] \times 1000$, where $R = {}^{65}Cu/{}^{63}Cu$) (Zhu et al. 2000). MC-ICP-MS measurements of Cu isotopic variations in natural samples with small analytical errors ($2\sigma = 0.05‰$) were first reported by Maréchal et al. (1999). Subsequently, many precise isotopic compositions of Cu were measured by MC-ICP-MS with analytical errors of typically 0.03‰–0.04‰ (1σ), for both Zn doped and sample standard bracketing (SSB) techniques (Zhu et al. 2000; Maréchal and Albarède 2002).

In this paper, we present new zinc-, copper-, and strontium-isotope data for sphalerite, tetrahedrite, chalcopyrite, and gangue minerals, collected from the eastern and western ore blocks in sediment-hosted, Cu–Ag–Pb–Zn polymetallic deposits of the Baiyangping ore district in western Yunnan, China. It's located in the northern part of the Lanping-Simao foreland fold belt, between the Jinshajiang-Ailaoshan and Lancangjiang Faults. This area is divided into eastern and western ore zones (Xu and Li 2003; He et al. 2005, 2009; Hou et al. 2007, 2008; Feng et al. 2011b), and is interpreted to have formed in a continental collision setting, controlled by thrust tectonics, in the strongly deformed Lanping sedimentary Basin (He et al. 2005, 2009; Hou et al. 2007, 2008; Xue et al. 2007). The area contains important reserves of Ag (4150 t), Cu (32.07 Mt), Pb (22.78 Mt), Zn (17.74 Mt), and Co (1444 t) (Third Geology and Mineral Resources Survey 2003). Previous studies of the Baiyangping district have examined the formation of the sedimentary basin, the structural evolution of the area, and the sources of ore metals and hydrothermal fluids (Tian 1997, 1998; Gong et al. 2000; Xue et al. 2002, 2003, 2007; Zhu et al. 2002; Shao et al. 2003; Wang and He 2003; Xu and Li 2003; Yang et al. 2003; Chen et al. 2004; He et al. 2004, 2005, 2006, 2009; Zhang 2005; Fan et al. 2006; Liu et al. 2010; Wang et al. 2011; Feng et al. 2011b), which demonstrates that these two ore blocks differ from common ore deposit models, such as magmatic-hydrothermal type, volcanic-hosted massive sulfide (VHMS), sedimentary exhalative (SEDEX) and typical Mississippi valley-type (MVT) deposits (He et al. 2005, 2009; Feng et al. 2011b).

The availability of detailed information on the geology, mineralogy, and geochemistry of the study area allows for an investigation of the variability in zinc, copper, and strontium isotopes within these deposits, and to identify the primary controls on any identified isotopic variation. In documenting and interpreting the first zinc, copper, and strontium isotope data for the two ore blocks, we use these data, in combination with previous research results, to discuss and elucidate the possible controls on the zinc, copper, and strontium variations during Pb–Zn mineralization, and sources of the various metals and fluids in an ore-deposit generation.

2 Geological setting

2.1 Regional geology and tectonic setting

The Sanjiang area in southwest China (Fig. 1a) is a tectonic belt located between the Tethyan-Alpine realm and the western Pacific and has experienced Proto-Tethyan, Paleo-Tethyan, and Meso-Tethyan phases of evolution (Li et al. 1991; Zhong and Ding 1993). The complexity of the structure of the crust in this area has created favorable conditions for mineralization (Chen 1991; Luo et al. 1994; Liao and Chen 2005; Hou et al. 2006, 2007, 2008).

The Mesozoic-Cenozoic Lanping Basin is an important part of the Sanjiang tectonic belt; it lies between the Lancangjiang and Jinshajiang Fault zones (Fig. 1b). The basin underwent a complex history of tectonic evolution, from Late Triassic rifting through Jurassic-Cretaceous subsidence and early Tertiary foreland development to final incorporation in the Lanping-Simao foreland fold belt (Wang et al. 2001), as a consequence of crustal shortening in eastern Tibet related to Indo-Asian collisional tectonics (Wang and Burchfiel 1997).

The Lanping Basin lies at the triple junction between the Eurasian, Indian, and Pacific plates, which is a complex tectonic environment that generated conditions favorable for the formation of the renowned Sanjiang polymetallic ore belt that is exceptionally enriched in copper (Chen 1991; Hou et al. 2008). The Baiyangping district is located in the northern part of the Lanping Basin. The eastern part of the basin is part of the Yangtze Plate, while the western part forms part of the Tibet-Yunnan Plate (Fig. 1b; Xue et al. 2007). Thrust-nappe systems are a significant deformation style in the Lanping fold belt, which resulted from Indo-Asian collision and subsequent oblique convergence during the Paleocene to Eocene. Two approximately E–W-striking geological cross-sections across the northern Lanping Basin show that the main thrust Faults dip to the west in the western segment and to the east in the eastern segment of the basin (He et al. 2009). The distributions of the eastern and western ore belts are governed by the thrust-napped system; the belts are associated with frequent tectonic and magmatic activity forming complex and diverse geological landscapes (Fig. 1c). The district shows multi-stage mineralization and a variety of ore-forming elements and petrological characteristics (Yin et al. 1990;

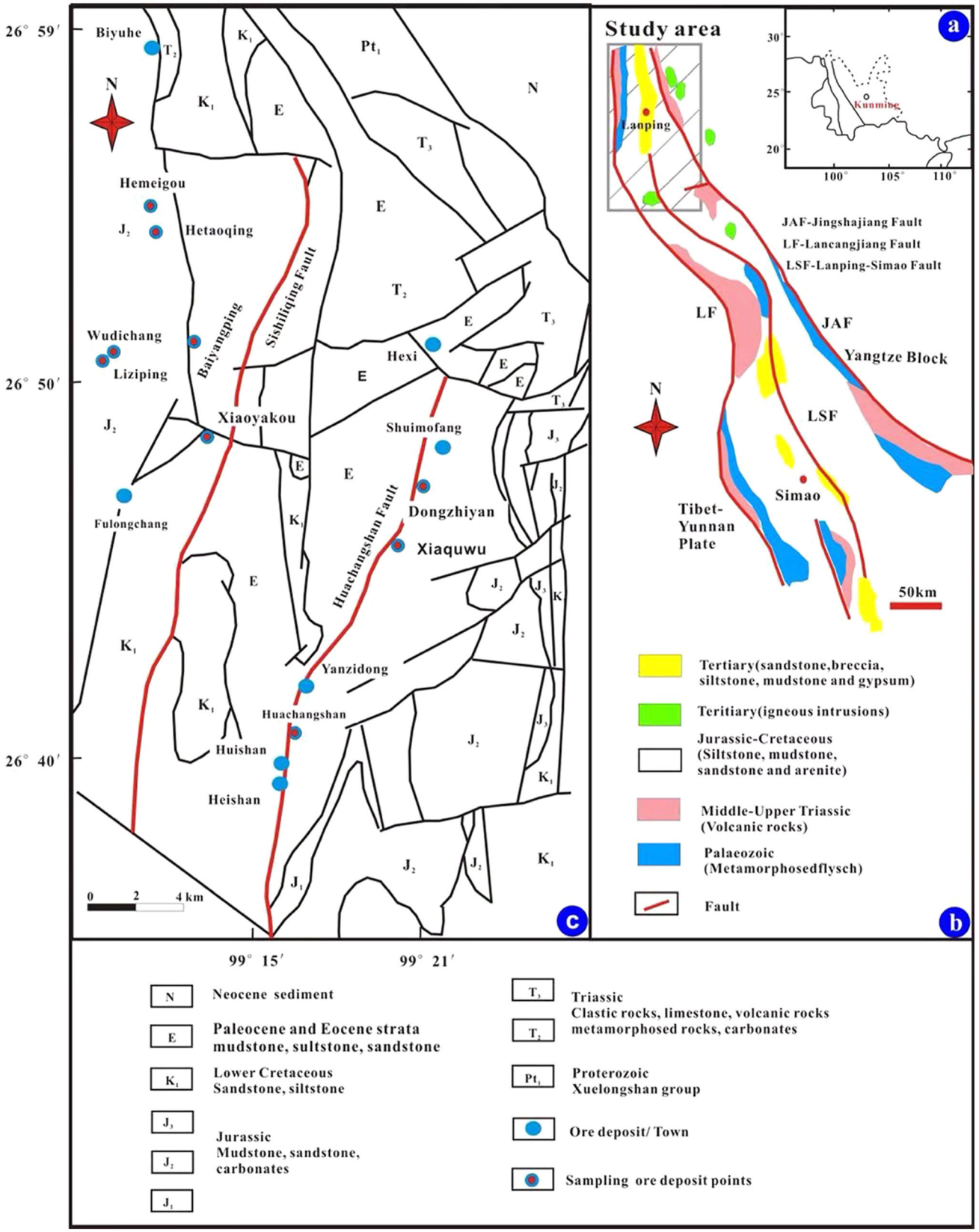

Fig. 1 **a** Map illustrating the location of the study area in southwest China; **b** tectonic location and geological sketch map of the Lanping basin highlighting the strata and faults present; **c** geological sketch map of the Baiyangping Cu–Pb–Zn–Ag polymetallic ore deposit, Lanping basin, southwestern China indicating the strata, faults present, and distribution of ore deposits (Xue et al. 2007; Feng et al. 2011b)

Tian 1997, 1998; Li et al. 1999; Chen et al. 2000; Yang et al. 2003; Xue et al. 2007; He et al. 2009).

2.2 Stratigraphy

The exposed strata in the Baiyangping mining district are Mesozoic and Cenozoic continental "red-bed" clastic formations. There are several sedimentary gaps in the stratigraphic column of the Lanping Basin (Qin and Zhu 1991; Xue et al. 2002). The basin is filled with siliciclastic rocks, except for the lowest part of the sequence and the Late Triassic Sanhedong Formation (T_3s), which consists mainly of fossiliferous marine limestone (Xue et al. 2002, 2006). The Mesozoic-Cenozoic strata that crop out in the ore district are summarized as follows (Fig. 2; Xue et al. 2002, 2006; He et al. 2009; Feng et al. 2011b): E_2g: Eocene Guolang Formation, comprising argillaceous sandstone, siltstone, and gypsum; E_1y: Paleocene Yunlong Formation, comprising breccia, sandstone, and gypsum in the upper part, and siltstone, mudstone, and gypsum in the lower part; K_2h: Middle Cretaceous Houtousi Formation, comprising quartz arenite and arkosic arenite; K_1j: Lower Cretaceous Jingxing Formation, comprising coarse-grained sandstone and arenite with coal seams and plant fossils; J_2h: Middle Jurassic Huakaizuo Formation, comprising siltstone and mudstone with abundant fossils; T_3m: Late Triassic Maichuqing Formation, comprising continental gray to black shale, siltstone, and fine-grained sandstone with local coal seams and plant fossils; T_3wl: Late Triassic Waluba Formation, comprising continental mudstone and siltstone; T_3s: Late Triassic Sanhedong Formation, comprising marine limestone and dolomitic limestone, and T_3w: Late Triassic Waigucun Formation, comprising conglomerate and sandy mudstone. The N_2s (Sanying Formation), N_2j (Jianchuan Formation), E_3, and J_1y (Yangjiang Formation) strata are absent within the Lanping Basin but occur in other areas in the Lanping-Simao fold belt (He et al. 2009).

2.3 Eastern ore zone

The eastern (or Sanshan-Hexi) ore zone is the second-largest ore district in the Lanping Basin and contains significant reserves of Cu (~ 0.3 Mt), Ag (> 3000 t), Pb + Zn (> 0.5 Mt), and Sr, with grades of 1.6%–3.3% Zn, 0.81%–3.55% Pb, and 23–220 g/t Ag (Third Geology and Mineral Resources Survey 2003; He et al. 2009). Fifteen economic ore bodies are located in the eastern ore zone, and these occur in the form of veins, lenses, weakly-stratified and irregularly-shaped bodies. The dimensions of these ore bodies are between 200 and 1000 m in length and between 2 and 8 m wide (Third Geology and Mineral Resources Survey 2003; Liu et al. 2010).

The eastern ore zone consists of the Hexi, Xiaquwu, Dongzhiyan, Yanzidong, Huishan, Heishan, and Huachangshan ore blocks that are distributed mainly along the Huachangshan thrust Fault (Fig. 1c). The belt generally dips to the east but locally dips to the west in the vicinity of the Dongzhiyan-Xiaquwu block. A fractured zone occurs in this block, being 10–20 m in width and exhibiting

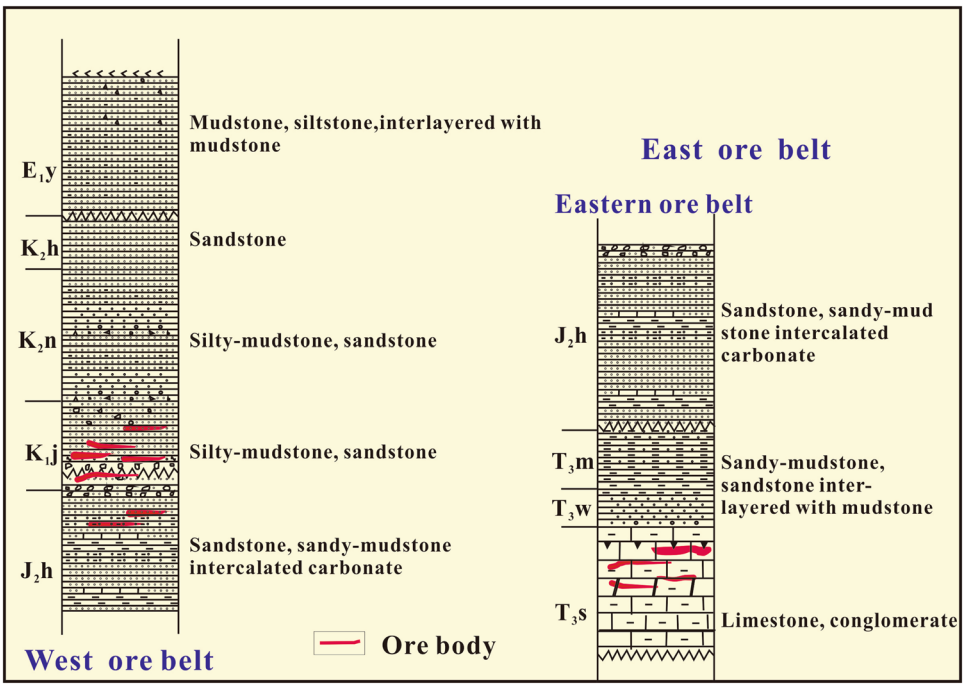

Fig. 2 Stratigraphic column for the Baiyangping Cu–Pb–Zn–Ag polymetallic ore deposit, Lanping basin, southwestern China (He et al. 2009)

lithological zoning, from an inner compressional schistose zone to an outer zone of fractured rock. Most of the ore blocks occur along the thrust fault and within zones of fracturing in the hanging-wall carbonate sequence (T_3s). Approximately E–W-trending strike-slip faults in the eastern thrust system commonly truncate the ore bodies, indicating that the faults postdate mineralization. The host sequence of the eastern ore zone consists of carbonates of the Late Triassic Sanhedong Formation (T_3s) and underlying sandstones of the Paleocene Yunlong (E_1y) and Eocene Baoxiangsi formations (E_2b). T_3s carbonates, a significant ore horizon, are composed of thick gray brecciated limestone, dolomitic limestone, and dolomite in the lower part, and gray brecciated siliceous limestone and muddy limestone in the upper part (Fig. 2). The upper carbonate sequence hosts ore bodies in the Huishan, Heishan, and Huachangshan blocks, whereas the lower carbonate sequence hosts ore bodies in the other ore blocks.

Alteration of the host rocks is dominated by dolomitization, calcification, and silicification. Alteration mineral assemblages consist of pyrite, barite, fluorite, calcite, celestite, dolomite, and minor quartz. Ore minerals include sphalerite, galena, pyrite (marcasite), and Cu-sulfides (tetrahedrite, Ag- and As-tetrahedrite, chalcocite, chalcopyrite, and bornite) with minor tenorite, cerussite, smithsonite, azurite, and covellite. Gangue minerals consist of calcite, celestite, siderite, dolomite, barite, fluorite, and minor quartz (Chen et al. 2000; He et al. 2009).

2.4 Western ore zone

The western (or Baiyangping-Fulongchang) ore zone is a large ore district in the Lanping Basin. The Baiyangping ore block contains reserves of Cu (0.22%–5.0%), while the Fulongchang ore block contains reserves of Ag (0.0041%–0.065%), Pb (1.0%–6.5%), and Cu (0.43%–4.20%) (Third Geology and Mineral Resources Survey 2003; Liu et al. 2010).

The western ore zone comprises the Baiyangping, Fulongchang, Wudichang, Liziping, Hetaoqing, Xiaoyakou, and Hemeigou ore blocks, which are distributed mainly along the Sishiliqing thrust Fault (Fig. 1c). Approximately NE-striking second-order faults, related to an N–S-striking thrust fault and an E–W-striking strike-slip fault in the western thrust system, commonly truncate the ore bodies. The Fulongchang ore block is dominated by Cu–Ag and is locally rich in Pb, Zn, and Co. Deposits include the Fulongchang (Baiyangping) Cu–Ag–Pb–Zn deposit, the Hetaoqing Cu–Ag deposit, and the Wudichang Zn–Pb–Ag deposit (Fig. 1b; He et al. 2009). The host sequence of the western ore zone consists of quartz sandstone, siltstone, and mudstone of the Early Cretaceous Jinxing Formation (K_1j), and mudstone, sandstone, and carbonate of the Middle Jurassic Huakaizuo Formation (J_2h) (Fig. 2).

Alteration of the host rocks is dominated by weak silicification and carbonatization. Alteration mineral assemblages are consisting of pyrite, barite, fluorite, calcite, celestite, dolomite, and minor quartz. Copper-bearing sulfides include tetrahedrite, arsenian tetrahedrite, Ag-bearing tetrahedrite, chalcopyrite, bornite, and chalcocite. Other sulfides are pyrite, pyrrhotite, sphalerite, and galena (He et al. 2009). Gangue minerals are dominated by quartz, with minor calcite, ankerite, barite, siderite, chlorite, and rare bitumen and graphite (Zhao 2006; He et al. 2009).

3 Sampling and analytical methods

3.1 Zn and Cu isotope samples

Samples for Zn isotope analyses were collected from the Sanhedong Formation (T_3s), in the Huangchangshan, Xiaquwu, and Dongzhiyan ore blocks in the eastern ore zone, and from the Huakaizuo (J_2h) and Jingxing (K_1j) formations in the Liziping, Wudichang, Hemeigou, Baiyangping, and Hetaoqing ore blocks, in the western ore zone of the Baiyangping ore district (Lanping, Yunnan Province, China) (Fig. 3). Two distinct stages of sphalerite mineralization from the eastern and western ore belts have been identified, based upon mineral paragenesis, textural and structural characteristics, and cross-cutting relationships. These are (1) early sphalerite: automorphic, hypidiomorphic, and xenomorphic granular textures are the main ore textures, and this sphalerite occurs as a disseminated ore (Fig. 3a, d) and; (2) late-stage sphalerite: sphalerite veins in calcite, automorphic granular texture, coarse-banded vein texture, and sphalerite cross-cutting earlier minerals (Fig. 3b, e). Samples for Cu isotope analyses were collected from the Huakaizuo (J_2h) and Jingxing (K_1j) formations in the Liziping, Wudichang, Hemeigou, Baiyangping, and Hetaoqing ore blocks in the western ore zone of the Baiyangping ore district (Lanping, Yunnan Province, China) (Fig. 4). Tetrahedrite and chalcopyrite are associated with ankerite and celestite veins. Automorphic/xenomorphic tetrahedrite occurs as disseminated ore and chalcopyrite occurs in veins cutting the tetrahedrite.

After petrographic observations, sulfide minerals (sphalerite, chalcopyrite, and tetrahedrite) from mineralization-stage rocks were trimmed to remove altered surfaces and then separated from their host rocks by crushing and handpicking. The picked samples were cleaned with deionized water and crushed and powdered in an agate mill. All samples were subsequently selected by handpicking under a binocular microscope. The identification of mineral phases was performed by electron probe

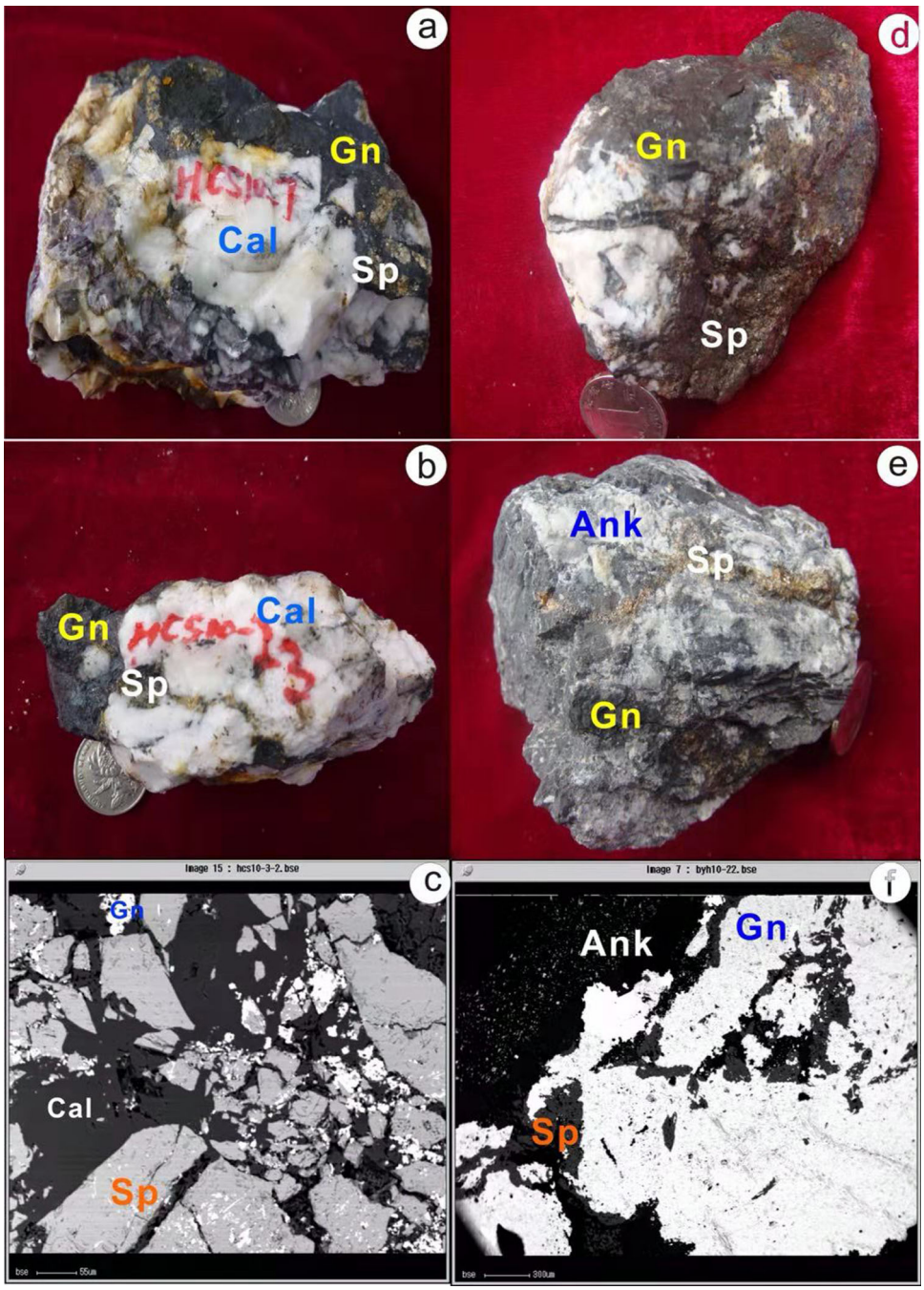

Fig. 3 Photos of sphalerite and galena ore samples and backscattered electron (BSE) images of ore in eastern and western ore belts. *Sp.* Sphalerite, *Gn.* Galena, *Cal.* Calcite, *Ank.* ankerite, **a–c** represent ore samples in the eastern ore belt, **d–f** represent ore samples taken from the western ore belt. **a** Early-stage sphalerite-massive Gn. + disseminated Sp. + vein Cal.; **b** late-stage sphalerite-massive Gn. + vein Sp. + massive Cal.; **c** BSE image of Gn. + Sp. + Cal.; **d** early-stage sphalerite-disseminated and massive Sp. + massive Gn. + massive Cal.; **e** late-stage sphalerite, massive Gn. + vein Sp. + massive Ank; **f** BSE image of Gn. + Sp. + Ank

microanalysis (Shimadzu EPMA-1600) at the State Key Laboratory of Ore Deposit Geochemistry, IGCAS.

3.2 Sr isotope samples

Samples for Sr isotope analyses were collected from the Sanhedong Formation (T3s) in the Huachangshan, Xiaquwu, and Dongzhiyan ore blocks within the eastern ore zone, and in the Liziping and Baiyangping ore blocks in the western ore zone of the Baiyangping ore district, Lanping, Yunnan Province, China. Samples were petrographically examined before gangue (calcite and dolomite), ore, and wall-rock samples were trimmed to remove altered surfaces, cleaned with deionized water, and crushed and powdered in an agate mill. Doubly polished calcite and dolomite thin sections were prepared from the selected samples and examined by standard microscopy before further analysis. The contents of Rb–Sr and Sr isotopic compositions were undertaken using thermal ionization mass spectrometry at the IGCAS.

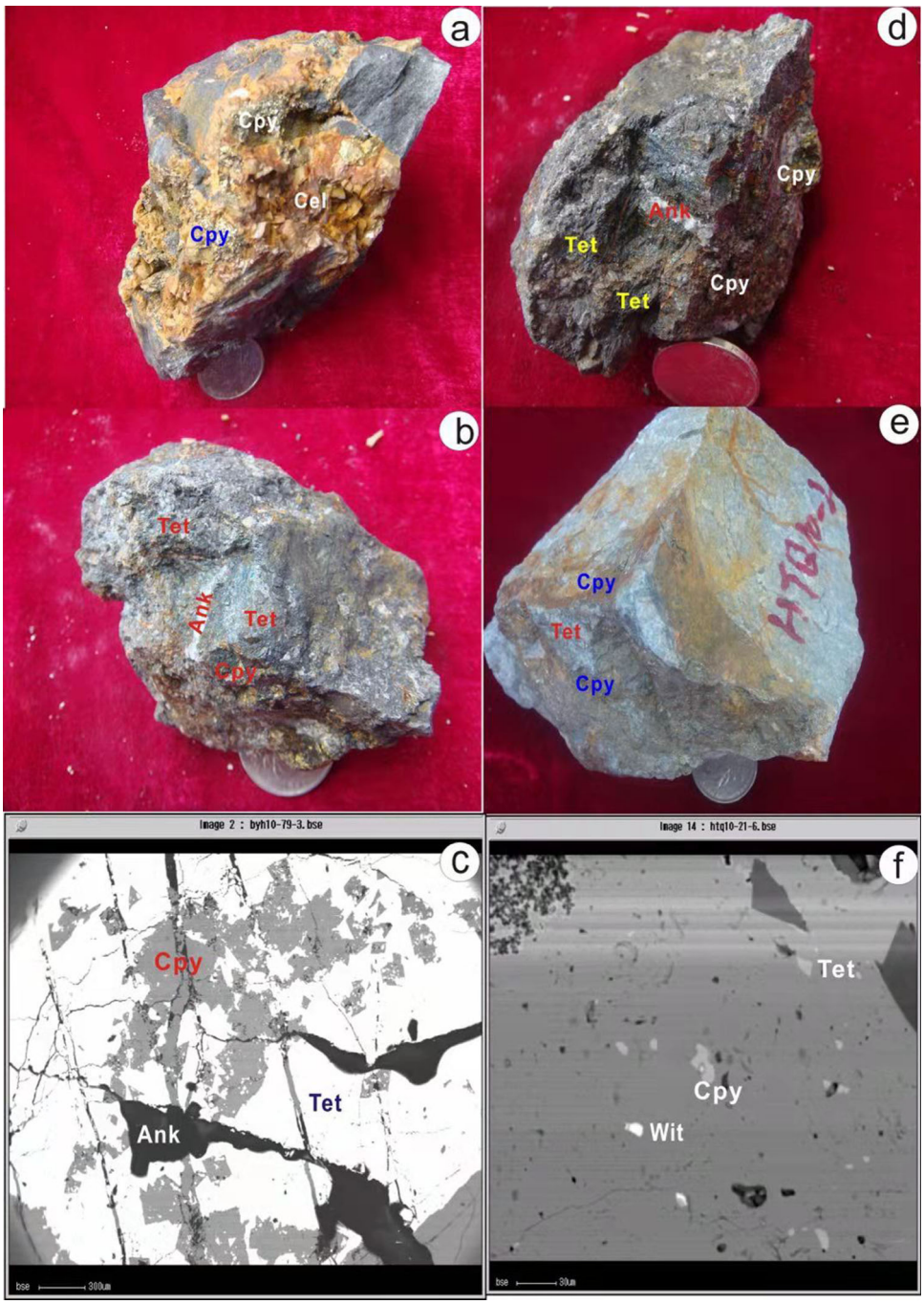

Fig. 4 Photos of chalcopyrite and tetrahedrite ore samples and BSE images of ore in the western ore belt. *Ccp.* chalcopyrite, *Cel.* celestite, *Tet.* tetrahedrite, *Cal.* calcite, *Ank.* ankerite, *Wit.* wittichenite. **a** Disseminated Cpy. + massive Cel.; **b** massive Tet. + vein Cpy. + vein Ank.; **c** BSE image of Cpy. + Tet. + Ank.; **d** massive Tet. + vein Cpy. + vein Ank.; **e** massive Tet. + vein Cpy.; **f** BSE image of Cpy. + Tet. + Wit

3.3 Copper, zinc, and strontium isotope measurements

Complete separation of Cu and Zn in sulfide samples was achieved using anion exchange chromatography. Resin AGMP-1 was used as the anion exchange resin, and 7 mol/L HCl for Cu and 0.5 mol/L HNO_3 for Zn were used as eluents. In this case, Cu and Zn can be well separated from Co and other elements, as sulfide samples have low contents of Na^+, Ca^{2+}, Mg^{2+}, and Al^{3+} (Tang et al. 2006b). The basic principle, the method of chemical separation, and the separation results of multi-element standard solutions and geological standard samples have been discussed previously (Tang et al. 2006b; Tang et al. 2006a). The copper and zinc isotope measurements were undertaken using a Nu Plasma (HR) MC-ICP-MS at the Isotope Geological Laboratory, Institute of Geology, Chinese Academy of Geological Sciences (IGCAGS), Beijing, China. The factors affecting mass discrimination are essential for mass bias correction during isotopic measurements using MC-

ICP-MS. We used the SSB (sample-standard bracketing) method relative to the NIST976 ($^{63}Cu/^{65}Cu = 2.24 \pm 0.0021$) copper standard for instrumental mass discrimination (Zhu et al. 2000; Cai et al. 2006; Li et al. 2008a, b). Due to the lack of reference standard of JMC-Lyon, IRMM-3702 is increasingly used as the Zn reference standard. And the difference can be calculated by$\delta^{66}ZnJMC\text{-}Lyon = \delta^{66}ZnIRMM\text{-}3702 + 0.28‰$ (Archer et al. 2017). So we used the $\delta^{66}ZnJMC\text{-}Lyon = 0.37441$ (Rosman 1972; Loss and Lu 1990), got the standard value of $\delta^{66}ZnIRMM\text{-}3702$ is 0.09441. It is proposed that HCl is a better medium than HNO_3 for sample introduction for Cu and Zn isotope measurements using MC-ICP-MS. The repeatability of $^{65}Cu/^{63}Cu$ and $^{66}Zn/^{64}Zn$ measurements in 0.1 mol/L HCl solution is 0.00008 (2σ), which is better than that for HNO_3 (Cai et al. 2006; Li et al. 2008a, b).

Strontium was extracted using cation exchange chromatography with 3 mol/L HNO_3. Strontium was leached from the crushed sample powders using a procedure modified by Simonetti (2008). Approximately 100 mg of powder was leached overnight in 4 mL of cold 0.6 N HCl in clean Savillex 15-mL beakers. The sample was transferred into a centrifuge tube and diluted to 10 mL with doubly distilled water and centrifuged for 10 min at 1000 rpm. The supernatant was then filtered through Qualitative No. 4 filter paper, evaporated to dryness and then re-dissolved in 1 mL of 2.5 N HCl. Samples were analyzed for strontium isotopic composition on a thermal ionization mass spectrometer. The total procedural blanks were 2–4 pg Sr and measurement of standard sample NBS987 yielded $^{87}Sr/^{86}Sr = 0.710262 \pm 7$.

4 Results

Zinc isotope data in samples from the western and eastern ore zones of the Baiyangping polymetallic ore district reveal the following. 1. The $\delta^{66}Zn$ value of sphalerite samples from the eastern ore zone ranged from − 0.09‰ to + 0.15‰, with a mean value of + 0.01‰. Sphalerite, which precipitated in the early and late mineralization stages of the eastern ore zone, yields $\delta^{66}Zn$ values of − 0.09‰ to − 0.02‰ and + 0.03‰ to + 0.15‰, respectively (Table 1). 2. The $\delta^{66}Zn$ value of sphalerite samples from the western ore zone (Liziping ore block) ranges from − 0.21‰ to − 0.01‰, with a mean value of − 0.12‰; only one sample gave a high value (+ 0.05‰). Two sphalerite samples from the Wudichang ore block gave $\delta^{66}Zn$ values of − 0.09‰ and + 0.04‰, with a mean value of − 0.03 ‰ (Table 1). Sphalerite, which precipitated during the early and late stages of mineralization in the western ore zone, yields $\delta^{66}Zn$ values of − 0.21‰ to − 0.09‰ and − 0.04‰ to + 0.05 ‰, respectively (Table 1).

Table 1 Zn isotopic composition of sphalerite in Baiyangping Cu–Pb–Zn–Ag polymetallic ore deposit, Lanping basin, southwestern China

No.s	Objects	Positions	Stages ORE	$\delta^{66}Zn$ (‰) BELT	SD
Eastern					
HCS10-7	Sp	Huachangshan	Early	− 0.09	0.02
HCS10-3-2	Sp	Huachangshan	Early	− 0.02	0.04
HCS10-21	Sp	Huachangshan	Early	− 0.06	0.01
HCS10-23	Sp	Huachangshan	Late	0.03	0.02
HCS10-14	Sp	Huachangshan	Late	0.15	0.03
HCS10-22	Sp	Huachangshan	Late	0.04	0.02
Western					
BYH10-10	sp.	Liziping	Early	− 0.21	0.02
BYH10-29	sp.	Liziping	Early	− 0.19	0.01
BYH10-30	sp.	Liziping	Early	− 0.17	0.03
BYH10-46	sp.	Wudichang	Early	− 0.09	0.01
BYH10-28	sp.	Liziping	Early	− 0.10	0.02
BYH10-17	sp.	Liziping	Late	− 0.04	0.04
BYH10-18	sp.	Liziping	Late	− 0.01	0.02
BYH10-19	sp.	Liziping	Late	0.05	0.02
BYH10-43	sp.	Wudichang	Late	0.04	0.01

Sp. = sphalerite; $\delta^{66}Zn$ values are given with the international error (2σ SD) for triplicate analysis of a single sample

SD standard deviation

Copper isotope data of the western ore zone of the Baiyangping polymetallic ore district yielded the following results. (1) The $\delta^{65}Cu$ value of chalcopyrite and tetrahedrite samples from the Hemeigou ore block ranged from − 0.20‰ to − 0.07‰ and from 0.00‰ to + 0.12‰, respectively. Only one tetrahedrite sample from the Wudichang ore block had a $\delta^{65}Cu$ value of + 0.05‰. (2) The $\delta^{65}Cu$ value of tetrahedrite and chalcopyrite samples from the Baiyangping ore block ranged from − 0.08‰ to − 0.06‰ and from − 0.72‰ to − 0.29‰, respectively; the $\delta^{65}Cu$ value of tetrahedrite samples from the Hetaoqing ore block ranged from − 0.02‰ to + 0.06‰ (Table 2). Of note, in the western ore zone, tetrahedrite precipitated in the early mineralization stage, whereas chalcopyrite precipitated in the late mineralization stage.

Table 2 Cu isotopic composition of chalcopyrite and tetrahedrite in Baiyangping Cu–Pb–Zn–Ag polymetallic ore deposit, Lanping basin, southwestern China

No.s	Objects	Positions	Stages	δ^{65}Cu (‰)	SD
BYH10-1	Cpy	Hemeigou	Late	− 0.12	0.01
BYH10-2	Cpy	Hemeigou	Late	− 0.20	0.03
BYH10-4	Cpy	Hemeigou	Late	− 0.16	0.02
BYH10-5	Cpy	Hemeigou	Late	− 0.07	0.02
BYH10-8	Cpy	Hemeigou	Late	− 0.08	0.04
BYH10-6-1	Tet	Hemeigou	Early	0	0.04
BYH10-07-2	Tet	Hemeigou	Early	0.12	0.02
BYH10-41	Tet	Wudichang	Early	0.05	0.02
BYH10-79	Cpy. + Tet	Baiyangping	Early	− 0.08	0.03
BYH10-82	Tet	Baiyangping	Early	− 0.06	0.01
BYH10-63	Cpy	Baiyangping	Late	− 0.72	0.03
BYH10-69	Cpy	Baiyangping	Late	− 0.41	0.02
BYH10-73	Cpy. + Tet	Baiyangping	Late	− 0.29	0.01
HTQ10-17	Tet	Hetaoqing	Late	− 0.02	0.02
HTQ10-30	Tet	Hetaoqing	Early	0.05	0.04
HTQ10-37	Tet	Hetaoqing	Early	0.06	0.03
HTQ10-4	Tet	Hetaoqing	Early	0.03	0.02

Cpy. chalcopyrite; *Tet.* tetrahedrite; δ^{65}Cu values are given with the international error (2σ SD) for triplicate analysis of a single sample

SD standard deviation

Table 3 Rb–Sr data and $^{87}Sr/^{86}Sr$ ratios analysis conducted on the calcite in Baiyangping Cu–Pb–Zn–Ag polymetallic ore deposit, Lanping basin, southwestern China

No.s	Objects	Rb (ppm)	Sr (ppm) ORE	Rb/Sr BELT	$^{87}Sr/^{86}Sr \pm 2\sigma$
Eastern					
HCS10-1-2	Calcite	0.046	352	0.0001	0.709116 ± 6
HCS10-14	Calcite	0.045	353	0.0001	0.709098 ± 8
HCS10-15	Calcite	0.085	352	0.0002	0.709213 ± 4
HCS10-19	Dolomitisationcalcite	0.139	406	0.0003	0.708020 ± 4
HCS10-22	Calcite	0.051	630	0.0001	0.709316 ± 6
HCS10-23	Calcite	0.042	348	0.0001	0.709344 ± 4
XQW10-33	Dolomitisationcalcite	0.177	274	0.0006	0.708689 ± 7
Western					
DZY10-48	Dolomitisationcalcite	0.185	1180	0.0002	0.707982 ± 17
BYH10-7	Calcite	0.194	108	0.0018	0.710856 ± 5
BYH10-15	Calcite	0.124	640	0.0002	0.708488 ± 4
BYH10-21	Calcite	0.502	8000	0.0001	0.711276 ± 7
BYH10-52	Calcite	0.161	69.1	0.0023	0.708803 ± 5

The strontium isotopic compositions of eight samples (calcite and dolomitized calcite) from the eastern and western ore zones are listed in Table 3. The value of $^{87}Sr/^{86}Sr$ in the eastern ore zone ranges from 0.7080 to 0.7093; the data show a trend of $^{87}Sr/^{86}Sr_{Huachangshan\ ore\ block} > {}^{87}Sr/^{86}Sr_{Xiaquwu\ ore\ block} > {}^{87}Sr/^{86}Sr_{Dongzhiyan\ ore\ block}$, the sole exception being dolomitized calcite sample HCS10-19 ($^{87}Sr/^{86}Sr = 0.7080$). The value of $^{87}Sr/^{86}Sr$ in the western ore zone ranges from 0.7085 to 0.7113, showing a greater spread than the range in the eastern ore zone.

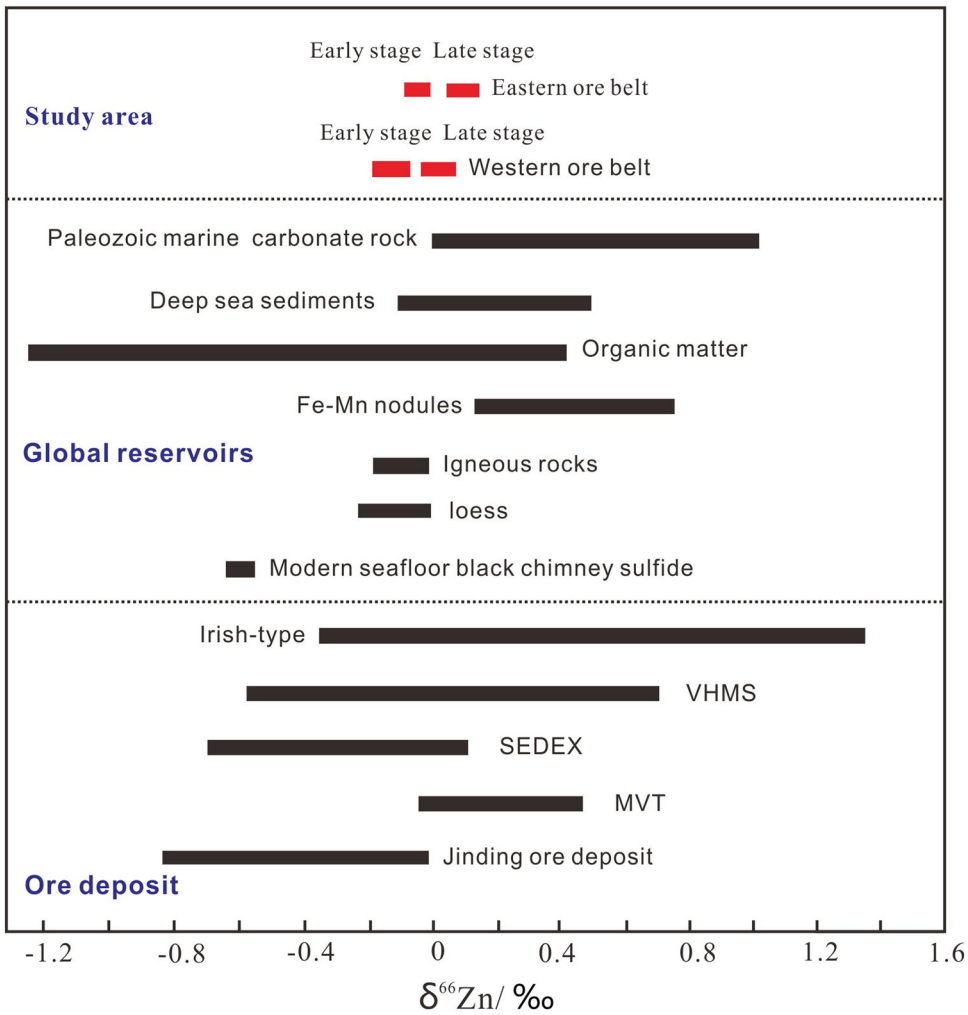

Fig. 5 Zn isotopic compositions for the various types of the ore deposit and for those from the study area (Maréchal et al. 1999, 2000; Helal et al. 2002; Pichats et al. 2003; Albarède 2004; Mason et al. 2005; Kelley et al. 2009; Gagnevin et al. 2012; Tang 2013)

5 Discussion

5.1 Zinc isotopes

Zinc isotopes have been used as tracers of (1) Biogeochemical and chemical processes (Maréchal et al. 2000; Zhu et al. 2002; Pichat et al. 2003; Pokrovsky et al. 2005; Bermin et al. 2006; Gelabert et al. 2006; Vance et al. 2006; Weiss et al. 2005); (2) The terrestrial rocks (Ben Othman et al. 2001, 2003, 2006); (3) Different sources of zinc (Maréchal et al. 1999, 2000; Helal et al. 2002) and (4) Climate change (Pichat et al. 2003). In addition, Zn isotopes have increasingly been used over the last decade in studies of different types of ore deposits and their genesis: e.g., the Alexandrinka volcanic-hosted massive sulfide deposit (Mason et al. 2005); the carbonate-hosted Zn–Pb deposits of the Irish Midlands ore field (Wilkinson et al. 2005; Crowther 2007); several modern submarine hydrothermal systems (John et al. 2008); the Red Dog shale-hosted base metal deposit (Kelley et al. 2009); several deposits in the Tongling area of Anhui, China (Wang and Zhu 2010); the world-class Navan Zn–Pb orebody, Ireland (Gagnevin et al. 2012); the Jinding Zn–Pb deposit of Yunnan, China (Tang 2013); Mississippi Valley-type carbonate-hosted zinc deposits in Cantabria, Spain (Pašava et al. 2014), and carbonate-hosted Pb–Zn sulfide deposits in southwest China (Zhou et al. 2014).

Based upon previous results, it is suggested that variations in zinc isotope compositions are controlled by three main factors: the temperature gradient (Mason et al. 2005), kinetic Rayleigh fractionation (John et al. 2008; Kelley et al. 2009; Maréchal and Sheppard 2002; Wilkinson et al. 2005; Gagnevin et al. 2012), and the mixing of multiple zinc sources (Wilkinson et al. 2005).

Sphalerite from the Baiyangping polymetallic ore district displays distinctly different Zn isotopic characteristics between the two ore zones. Samples from the eastern ore zone are enriched in heavy isotopic zinc, whereas samples from the western ore zone are enriched in light zinc (Table 1; Fig. 3, 5). Two types of aqueous fluids in these two ore zones have been identified from fluid inclusion studies (Xu and Li 2003; Chen et al. 2004; He et al. 2009;

Feng et al. 2014). The range in homogenization temperature (Th) values for these fluids is 92 to 283 °C (mean 152 °C, peak values at 130–140 °C) for the western ore zone, and 101 to 295 °C (with averages of 158.6 °C for calcite, 176.8 °C for dolomite, 162.2 °C for dolomitized limestone, 151.9 °C for Celestine, 172.3 °C for quartz, and 145.6° C for sphalerite, peak values at 120–200 °C) for the eastern ore zone (Feng et al. 2014). The mean Th values generally display an increase from the western to the eastern ore zones. Pašava et al. (2014) concluded that high Zn isotope values are consistent with the rapid precipitation of sphalerite from Zn–Cl species at higher temperatures, while low Zn isotope values result from the fractionation of aqueous Zn sulfide species at lower temperature and higher pH. It is noted that the high Zn isotope values have not resulted from temperature but the Zn-complexes. Just like Fujii et al.(2011) suggested that sulfides precipitating from hydrothermal solutions should be isotopically lighter than the solution, but the extent of isotope fractionation decreases with temperature. Maréchal and Sheppard (2002) conducted zinc isotope fractionation experiments at different temperatures. The α (fractionation factor) values of $ZnCl_2$ and Zn $(NO_3)_2$ are nearly equal to 1.00004 and 1.00011(the reaction of $ZnCl_2$ and Zn $(NO_3)_2$ with calcite at 30 °C and 50 °C, respectively), indicating that the change of temperature has no obvious effect on the fractionation of Zn isotopes. Therefore, although there is a temperature gradient variation between the western and eastern ore zones, whether the temperature has an effect on Zn isotope fractionation needs to be further studied in this paper.

The increased δ^{66}Zn values from the early to late-stage resulted from the Rayleigh fractionation of zinc isotopes. During fluid evolution in a hydrothermal system, the fluid becomes enriched in heavier Zn isotopes with the precipitation of minerals, and the Zn isotope composition of late-stage minerals is heavier than that of early-stage minerals (Archer et al. 2004; Mason et al. 2005; Wilkinson et al. 2005; John et al. 2008; Kelley et al. 2009; Wang and Zhu 2010; Gagnevin et al. 2012). Sphalerites from both ore zones show such a trend in zinc isotope evolution (Fig. 5), indicating that Rayleigh fractionation likely occurred. This process has been used to explain the variations in zinc isotopes in several deposits, including the Alexandrinka deposit (VHMS-type: − 0.03‰ to + 0.23‰; Mason et al. 2005), the Irish Midlands deposit (Irish-type: − 0.18‰ to + 0.64‰; Wilkinson et al. 2005), the Red Dog deposit (SEDEX-type: 0‰ to + 0.60‰; Kelley et al. 2009), the Navan deposit (Irish-type: − 0.32‰ to + 0.23‰; Gagnevin et al. 2012), the Jinding Zn–Pb ore deposit in Yunnan, China (− 0.85‰ to + 0.05‰; Tang 2013), and carbon-hosted Pb–Zn sulfide deposits in southwest China (− 0.26‰ to + 0.58 ‰ and + 0.07‰ to + 0.71‰, respectively; Zhou et al. 2014) (Fig. 5). Thus, Rayleigh fractionation is likely to have been the additional factor controlling the observed temporal and spatial (Fig. 5) variations in zinc isotopes in the two studied ore zones. Due to the obvious overlap of isotope data between different types of deposit, it is further suggested that the zinc isotopic composition (Table 1; Fig. 5) in the Baiyangping polymetallic Pb–Zn deposits may have the same fractionation as that of magmatic-hydrothermal, VHMS, SEDEX, and MVT deposits, as demonstrated by geological and other geochemical evidence (He et al. 2009; Feng et al. 2014).

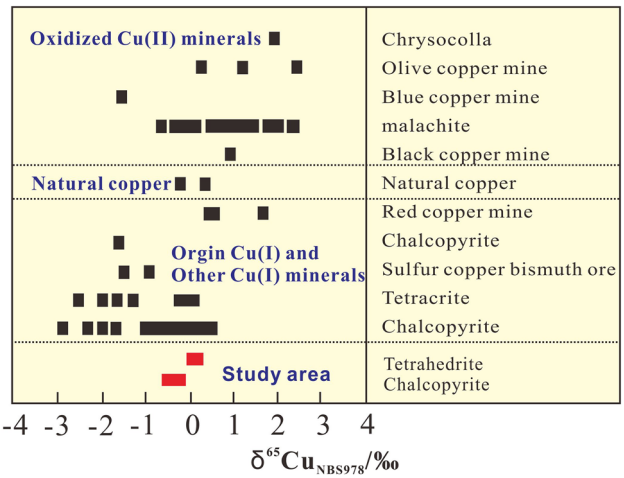

Fig. 6 Ranges of copper isotope data for different valence copper minerals (Markl et al. 2006)

5.2 Copper isotopes

Copper isotopes have been used to study significant Cu isotopic variations in soils (Bigalke et al. 2010, 2011; Liu et al. 2014); bacteria-metal interactions in natural waters, soils, and rocks as well as isotope fractionation during adsorption onto metal oxy-hydroxides and kaolinite (Balistrieri et al. 2008; Pokrovsky et al. 2008; Navarrete et al. 2011; Liu et al. 2014; Li et al. 2015); modern black smokers (Zhu et al. 2000; Rouxel et al. 2004; Berkenbosch et al. 2015); redox weathering of Cu-bearing sulfides (Mathur et al. 2012); massive sulfide deposits (Mason et al. 2005); porphyry copper deposits (Graham et al. 2004; Mathur et al. 2005, 2009; Li et al. 2010); skarns (Graham et al. 2004; Maher and Larson 2007); sedimentary copper mineralization (Asael et al. 2007), and other hydrothermal ore deposits (Jiang et al. 2002; Larson et al. 2003; Markl et al. 2006).

The natural variations in copper isotope ratios have been attributed to a number of processes, including liquid–vapor separation, multi-step equilibrium processes, redox reactions, physicochemical parameters (Eh, pH, and

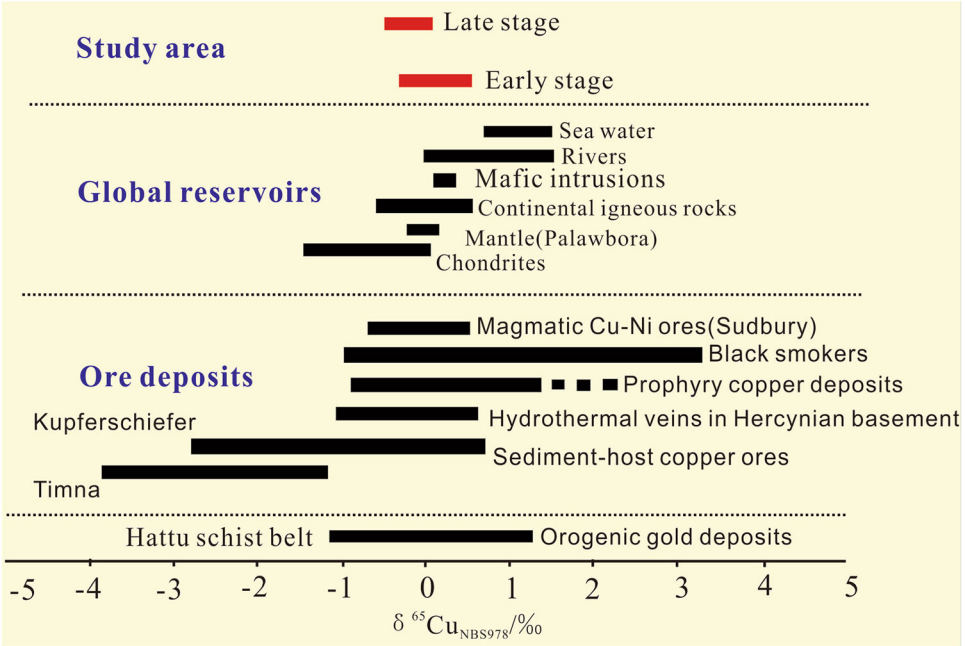

Fig. 7 Ranges of copper isotope data for global reservoirs, as well as for different types of ore deposits and those of the study area (Larson et al. 2003; Markl et al. 2006; Maher et al. 2007; Asael et al. 2007; Li et al. 2010; Ferenc et al. 2016)

temperature), and the involvement of organisms (Maréchal et al. 1999; Zhu et al. 2000, 2002; Jiang et al. 2002; Larson et al. 2003; Ehrlich et al. 2004; Graham et al. 2004; Rouxel et al. 2004; Asael et al. 2007; Mathur et al. 2009). Different types of deposit show distinct changes in the isotopic composition of copper: for example, high-temperature hydrothermal deposits generally show a narrow range of δ^{65}Cu values (Zhu et al. 2000; Jiang et al. 2001; Jiang 2003; Albarède 2004; Markl et al. 2006); epithermal and sedimentary deposits are characterized by low values of δ^{65}Cu and a somewhat restricted range (− 3.7‰ to + 0.5‰) (Jiang et al. 2001, 2002; Jiang 2003; Qian et al. 2006; Asael et al. 2007); and the oxidation of ore leads to a wide range of δ^{65}Cu values (− 3.4‰ to + 2.41‰) (Markl et al. 2006; Asael et al. 2007).

Massive tetrahedrite from the western ore zone, which precipitated during the early ore-forming stages, shows δ^{65}Cu values (− 0.06‰ to + 0.12‰) that are heavier than those of vein chalcopyrite (− 0.72‰ to − 0.07‰), which formed during the late ore-forming stages. In Fig. 6, we can see the most typical range of $\delta^{65}Cu_{NBS978}$ values for hypogene chalcopyrite from magmatic sulphide ores, intrusion-related hydrothermal systems (e.g., porphyry copper and base metal skarn ores), granite-related and non-magmatic polymetallic vein deposits, and sediment-hosted copper ores. Determined Cu isotope values for samples from the study area fall within the field for sediment-hosted copper ores (Fig. 7). Cu(0), Cu(I), and Cu(II) minerals occur across the globe. Although the valence of Cu in chalcopyrite has been the subject of much debate, the most recent mineralogical studies suggest that the valence state of most Cu in chalcopyrite is Cu(I) (Goh et al. 2006; Pearce et al. 2006). Fractionation between Cu(I) in minerals (e.g., chalcopyrite) and aqueous Cu(II) in leachate can be as high as 2.7‰ (Zhu et al. 2002; Ehrlich et al. 2004; Mathur et al. 2005; Kimball et al. 2009). Given that the samples of the present study are for chalcopyrite and tetrahedrite, which are both Cu(I) minerals (Fig. 6), and δ^{65}Cu values of tetrahedrite (− 0.06‰ to + 0.12‰) are heavier than those of vein chalcopyrite (− 0.72‰ to − 0.07‰), our data suggests that different minerals with the same valence can display evidence for isotopic fractionation. In addition, previous studies have shown that the fractionation of copper isotopes between different coexisting sulfide minerals can be up to 0.4‰ in moderate- to high-temperature porphyry deposits (Larson et al. 2003; Graham et al. 2004). The influence of fractionation between different copper-bearing minerals should be considered for the sake of rigorous logic in the discussion, even though the values may not be large.

Different stages of mineralization are characterized by dissimilar Cu isotopic contents (Zhu et al. 2000; Jiang et al. 2001; Harson et al. 2003; Rouxel et al. 2004; Mason et al. 2005). Copper sulfides that formed in the early stages are rich in ^{65}Cu whereas those that precipitated from late-stage fluids are commonly ^{65}Cu-depleted. Supergene Cu minerals yield a wide range of δ^{65}Cu values (− 8.4‰ to + 9.1‰), with a general shift towards isotopically heavy compositions, as compared with the inferred precursor minerals (Mason et al. 2005). The Cu isotope contents of chalcopyrite and tetrahedrite from the western ore zone show such a trend in copper isotope evolution (Fig. 7),

indicating that the difference in Cu isotopes could have developed in different ore-forming stages. Experimental studies show that ^{65}Cu tends to be transferred into minerals from solution (Pekala et al. 2011; Gregory and Mathur 2017); therefore, the Cu isotopic composition of the solution and minerals will increase as the reaction proceeds. However, the δ^{65}Cu values decrease from the early stage to the late stage in the western ore belt, which may be caused by the mixture of ore-forming fluids with different δ^{65}Cu values. This process has been used to explain variations in copper isotopes in several deposits, such as black smoker sulfide chimneys on the ocean floor (Zhu et al. 2000); the large isotopic variations in Cu (δ^{65}Cu from − 3.70‰ to + 0.30‰) observed in a sediment-hosted hydrothermal vein-type deposit from Jinman, China (Jiang et al. 2002); variations in copper isotopes in magmatic and hydrothermal ore-forming environments (Larson et al. 2003); and variations in copper isotopes in the Alexandrinka volcanic-hosted massive sulfide deposit (Mason et al. 2005). In addition, it has been shown that post-mineralization leaching can be significantly modifying the Cu isotopic data (Larson et al. 2003; Graham et al. 2004). Hence, alteration or leaching process should also be involved, same as to the description of microscopical photographs (Fig. 4c, f). Thus; different ore-forming stages and alteration or leaching process are likely the main factors controlling the observed (Fig. 7) variations in copper isotopes in the western ore zone.

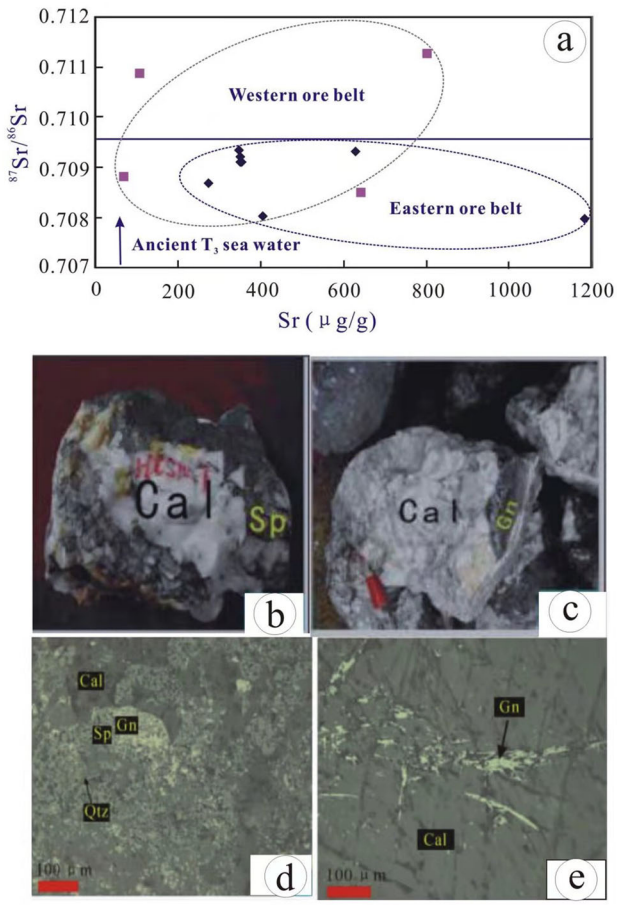

Fig. 8 **a** Sr isotopic composition of calcite from the Baiyangping Cu–Pb–Zn–Ag polymetallic ore deposit, Lanping Basin, southwestern China; **b** massive Cal. + Sp. (Huachangshan ore block, eastern ore belt); **c** massive Cal. + Gn. (Liziping ore block, western ore belt); **d** wide-vein Cal. microscopic image, symbiosis with Sp. + Gn. + Qrz. **e** massive Cal. Microscopic image, symbiosis with Gn. *Cal.* Calcite, *Sp.* Sphalerite, *Gn.* Galena, *Qrz.* quartz

5.3 Strontium isotopes

Numerous studies have shown that Sr-isotope ratios (e.g., ^{87}Sr/^{86}Sr) can be used to constrain the source of ore fluids. Studies of the isotopic composition of Sr in Sr-bearing minerals (e.g., calcite, fluorite, and dolomite) not only may help to determine the source of ore elements but also can provide important constraints on the genesis of hydrothermal deposits (Kesler et al. 1983; Lange et al. 1983; Norman and Landis 1983; Barbieri et al. 1987; Galino et al. 1994; Fanlo et al. 1998; Savard et al. 2000; Peng et al. 2001).

Rb cannot substitute for Ca^{2+} in the calcite lattice, in contrast to Sr, which shows limited substitution that leads to very small Rb/Sr ratios in calcite (Deer et al. 1966). Consequently, the composition of ^{87}Sr (decayed from Rb) has little impact on the initial Sr isotopic composition. It is then reasonable to assume that the ^{87}Sr/^{86}Sr ratio in calcite is the initial Sr isotopic composition of the ore-forming fluid from which the calcite precipitated (Kesler et al. 1983; Lange et al. 1983; Norman and Landis 1983; Barbieri et al. 1987; Galino et al. 1994; Fanlo et al. 1998; Savard et al. 2000; Peng et al. 2001).

Since the residence time of strontium in seawater (2–4 Myr) is much longer than the mixing time of seawater ($\sim 1.5 \times 10^3$ a), it is considered that the distribution of strontium isotopes in seawater is uniform (Brannon et al. 1991). The precipitated carbonate minerals in seawater show no significant Sr isotopic fractionation, and the Sr isotopic composition of carbonate minerals is consistent with that of seawater (Viezer 1989). Therefore, the ^{87}Sr/^{86}Sr ratio in the Late Triassic Sanhedong Formation carbonate rocks should be similar to that of Late Triassic seawater (0.7076–0.7078) (Korte et al. 2003). The ^{87}Sr/^{86}Sr values of hydrothermal calcite from both the eastern and western ore zones are nevertheless much higher than the value of Late Triassic seawater but are consistent with those of hydrothermal calcite from the Jinding Pb–Zn deposit (Fig. 8a, 0.7078–0.7119, Luo et al. 1994; 0.7097–0.7104, Tang 2013). The high ^{87}Sr/^{86}Sr value of hydrothermal calcite may, therefore, be related to

recrystallization (Fig. 8b, c, d, e) from a radiogenic Sr-rich or silicifying fluid, either from the strata that the ore-forming fluid flows through or from other fluids (Savard et al. 2000).

6 Conclusions

1. The zinc isotopic composition in the Baiyangping polymetallic Pb–Zn deposits may have the same fractionation as that of magmatic-hydrothermal, VHMS, SEDEX, and MVT deposits, as demonstrated by geological and other geochemical evidence.
2. The δ^{65}Cu values of early-stage massive tetrahedrite from the western ore zone are from − 0.06‰ to + 0.12‰, heavier than those of vein chalcopyrite (from − 0.72‰ to − 0.07‰) that formed during the late ore-forming stage. Different ore-forming stages and alteration or leaching process are likely the main factor controlling the observed variations in copper isotopes in the western ore zone.
3. The $^{87}Sr/^{86}Sr$ values of hydrothermal calcite in both the eastern and western ore zones suggest that the initial $^{87}Sr/^{86}Sr$ values of early calcite were much higher than the value of Late Triassic seawater, which may be related to recrystallization from a radiogenic Sr-rich or silicifying fluid, either from the strata that the ore-forming fluid flows through or from other fluids.

Acknowledgements We are grateful to Prof. Zhu XK for guidance and help during Cu, Zn isotope experiments. This research was financially supported by General Project of Natural Science Foundation of Shaanxi Province (2020JM-423).

References

Albarède F (2004) The stable isotope geochemistry of copper and zinc. Rev Mineral Geochem 55:409–427

Alvaro F, David MB (2009) Fractionation of Cu, Fe, and Zn isotopes during the oxidative weathering of sulfide-rich rocks. Chem Geol 264:1–12

Archer C, Vance D (2004) Mass discrimination correction in multiple-collector plasma source mass spectrometry: an example using Cu and Zn. J Anal Atom Spectrom 19:656–665

Archer C, Vance D, Butler I (2004) Abiotic Zn isotope fractionations associated with ZnS precipitation. Geochim Cosmochim Acta 68:A325

Archer CMB, Andersen C, Cloquet TM, Conway S, Dong M, Ellwood R, Moore J, Nelson M, RehkAmper O, Rouxel M, Samanta K-C, Shin Y, Sohrin S, Takano S, Wasylenki L (2017) Inter-calibration of a proposed new primary reference standard AA-ETH Zn for zinc isotopic analysis. J Anal At Spectrom 32(2):415–419

Asael D, Matthews A, Bar-Matthews M, Halicz L (2007) Copper isotope fractionation in sedimentary copper mineralization (Timna Valley, Israel). Chem Geol 243:238–254

Balistrieri LS, Borrok DM, Wanty RB, Ridley WI (2008) Fractionation of Cu and Zn isotopes during adsorption onto amorphous Fe(III) oxyhydroxide: experimental mixing of acid rock drainage and ambient river water. Geochim Cosmochim Acta 72:311–328

Barbieri M, Bellanca A, Neri R (1987) Use of strontium isotopes to determine the sources of hydrothermal fluorite and barite from Northwestern Sicily (Italy). Chem Geol 66:273–278

Barrett TJ, Anderson GM (1988) The solubility of sphalerite and galena in 1–5m NaCl solutions to 300 °C. Geochim Cosmochim Acta 52:813–820

Belogub EV, Novoselov CA, Spiro B, Yakovleva BA (2003) Mineralogical and S isotopic features of the supergene profile of the Zapadno-Ozernoe massive sulphide and Au bearing gossan deposit, South Urals. Mineral Mag 67:339–354

Ben Othman D, Luck JM, Grousset FE, Rousseau D, Albarede F (2001) Cu, Zn (and Pb) isotopes in aerosols and loesses. 11th European Geosciences Union Conference, p. 688

Ben Othman D, Luck JM, Tchalikian JM, Albarede F (2003) Cu-Zn systematics in terrestrial basalts. Geophys Res Abs 5:9669

Ben Othman D, Luck JM, Bodinier JL, Arndt NT, Albarede F (2006) Cu–Zn isotopic variations in the Earth's mantle. Geochimica et Cosmochimica Acta 70:A46

Berkenbosch HA, de Ronde CEJ, Paul BT, Gemmell JB (2015) Characteristic of Cu isotopes from chalcopyrite-rich black smoker chimneys at Brothers volcano, Kermadec arc, and Niuatahi volcano. Lau basin Miner Deposita 50:811–824

Bermin J, Vance D, Archer C, Statham PJ (2006) The determination of the isotopic composition of Cu and Zn in seawater. Chem Geol 226:280–297

Bigalke M, Weyer S, Kobza J, Wilcke W (2010) Stable Cu and Zn isotope ratios as tracers of sources and transport of Cu and Zn in contaminated soil. Geochim Cosmochim Acta 74:6801–6813

Bigalke M, Weyer S, Wilcke W (2011) Stable Cu isotope fractionation in soils during oxic weathering and podzolization. Geochimica et Cosmochimica Acta 75:3119–3134

Blix R, Ubisch HV, Wickman FE (1957) A search for variations in the relative abundance of the zinc isotopes in nature. Geochim Cosmochim Acta 11:162–164

Brannon JC, Podosek FA, Viets JG (1991) Strotium isotopic constraints on the origin of ore-forming fluids of the Viburnum Trend, Southeast Missouri. Geochim Cosmochim Acta 55:1407–1419

Buckley AN, Woods R (1984) An X-ray photoelectron spectroscopy study of the oxidation of chalcopyrite. Aust J Chem 37:2403–2413

Cai JJ, Zhu XK, Tang SH, Li SZ, He XX (2006) Assessment of interference in Cu isotope ratio measurements using multiple-collector inductively coupled plasma source mass spectrometry. Geol J China Univ 12:392–397 (**in Chinese with English abstract**)

Chapman JB (2006) Chemical separation and isotopic variations of Cu and Zn from five geological reference materials. Geostand Geoanal Res 30:5

Chen BW, Li YS, Qu JC (1991) The relationship between the main tectonic and metallogenic relations in Sanjiang Region. Geological Publishing House, Beijing, pp 30–40 (**in Chinese**)

Chen KX, He LQ, Yang ZQ, Wei JQ, Yang AP (2000) Oxygen and carbon isotope geochemistry in Sanshan-Baiyangping copper-silver polymetallogenic enrichment district, Lanping, Yunnan. Geol Miner Resour South China 16:1–8 (**in Chinese**)

Chen KX, Yao SZ, He LQ, Wei JQ, Yang AP, Huang HL (2004) Ore-forming fluid in Baiyangping silver-polymetallic mineralization

concentration field in Lanping, Yunnan Province. Geol Sci Tech Inf 23:45–50 (**in Chinese with English abstract**)

Crowther HL (2007) A rare earth element and transition metal isotope study of the Irish Zn–Pb orefield. published Ph.D. thesis, University of London, p 198

Deer WA, Howie RA, Russman J (1966) An introduction to the rock-forming minerals. Longman Scientific and Technical, New York, pp 511–515

Ehrlich S, Butler I, Halicz L, Rickard D, Oldroyd A, Matthews A (2004) Experimental study of copper isotope fractionation between aqueous Cu and covellite. CuS Chem Geol 209:259–269

Fan SJ, Wang AJ, Liu HB, Xiu QY, Cao DH, Li RP, Cao H, Chen QS (2006) A discussion on the helium and argon isotopic evidences for genesis of the Baiyangping copper-cobalt deposit in the Lanping basin. Geol Rev 52:628–635 (**in Chinese with English abstract**)

Fanlo I, Touray JC, Subías I (1998) Geochemical patterns of a shear fluorite vein, Parzan, Spanish Central Pyrenees. Miner Deposita 33:620–632

Feng CX, Bi XW, Hu RZ, Liu S, Wu LY, Tang YY, Zou ZC (2011a) Study on paragenesis-separation mechanism and source of ore-forming element in the Baiyangping Cu–Pb–Zn–Ag polylmetallic ore deposit, Lanping basin, southwestern China. Acta Petrologica Sinica 27:2609–2624 ((**in Chinese with English abstract**))

Feng CX, Bi XW, Wu LY, Zou ZC, Tang YY (2011b) Significance and characteristics of REE geochemistry in calcite in the Eastern ore belt of the Baiyanpin poly-metallic metallogenic province, northwestern Yunnan Province, China. J Jilin Univ 41:1397–1406 (**in Chinese with English abstract**)

Feng CX, Bi XW, Liu S, Hu RZ (2014) Fluid inclusion, rare earth element geochemistry, and isotopic characteristics of the eastern ore zone of the Baiyangping polymetallic Ore district, northwestern Yunnan Province. China J Asian Earth Sci 85:140–153

Ferenc M, Irmeli M, Hugh OB, Yann L, Lassi P, Bo J, Asko K, Peter S, Martin W, Grigorios S (2016) Boron, sulphur and copper isotope systematics in the orogenic gold deposits of the Archaean Hattu schist belt, eastern Finland. Ore Geol Rev 77:133–162

Fujii T, Moynier F, Pons ML, Albarede F (2011) The origin of Zn isotope fractionation in sulfides. Gechim Cosmochim Acta 75:7632–7643

Gagnevin D, Boyee AJ, Barrie CD, Menuge JF, Blakeman RJ (2012) Zn, Fe and S isotope fractionation in a large hydrothermal system. Gechim Cosmochim Acta 88:183–198

Gale NH, Woodhead AP, Stos-Gale ZA, Walder A, Bowen I (1999) Natural variations detected in the isotopic composition of copper: possible applications to archaeology and geochemistry. Int J Mass Spectrom 184:1–9

Galino C, Tornos F, Darbyshire DPF (1994) The age and origin of the barite-fluorite veins of the Sierra del Guadarrama: a radiogenic and stable isotope study. Chem Geol 112:351–364

Gelabert A, Pokrovsky O, Viers J, Schott J, Boudou A, Feurtet-Mazel A (2006) Interaction between zinc and freshwater and marine diatom species: surface complexation and Zn isotope fractionation. Geochimica et Cosmochimica Acta 70:839–857

Goh SW, Buckley AN, Lamb RN, Rosenberg RA, Moran D (2006) The oxidation states of copper and iron in mineral sulfides, and the oxides formed on initial exposure of chalcopyrite and bornite to air. Gechim Cosmochim Acta 70:2210–2228

Gong WJ, Tan KX, Li XM, Gong GL (2000) Geochemical characteristics of fluid and mechanism for ore formation in the Baiyangping copper-silver deposit, Yunnan. Geotectonica et Metallogenia 24:175–181 (**in Chinese with English abstract**)

Graham S, Pearson N, Jackson S, Griffin W, Reilly SYO (2004) Tracing Cu and Fe from source to porphyry: in situ determination of Cu and Fe isotope ratios in sulfides from the Grasberg Cu–Au deposit. Chem Geol 207:147–169

Greenwood NN, Whitfield HJ (1968) Mössbauer effect studies on cubanite ($CuFe_2S_3$) and related iron sulphides. J Chem Soc A Lond 7:1697–1699

Gregory MJ, Mathur R (2017) Understanding copper isotope behavior in the high temperature magmatic-hydrothermal porphyry environment. Geochem Geophys Geosyst 18:4000–4015

Hackl RP, Dreisinger DB, Peters E, King JA (1995) Passivation of chalcopyrite during oxidative leaching in sulfate media. Hydrometallurgy 39:25–48

Haest M, Muchez P, Petit JCJ, Vanhaecke F (2009) Cu isotope ratio variations in the Dikulushi Cu–Ag deposit, DRC: of primary origin or induced by supergene raw or king? Econom Geol 104:1055–1064

Halliday AN, Lee D-C, Christensen JN, Walder AJ, Freedman PA, Jones CE, Hall CM, Yi W, Teagle D (1995) Recent developments in inductively coupled plasma magnetic sector multiple collector mass spectrometry. Int J Mass Spectrom 146–147:21–33

He MQ, Liu JJ, Li CY, Li ZM, Liu YP (2004) Mechanism of Ore-Forming Fluids of the Lanping Pb-Zn-Cu polymetallic mineralized concentration Area. In: An example study on the Baiyangping Ore district. Geological Publishing House, Beijing, pp 1–117 (**in Chinese**)

He LQ, Chen KX, Wei JQ, Yu FM (2005) Geological and geochemical characteristics and genesis of ore deposits in eastern ore belt of Baiyangping area, Yunnan Province. Mineral Deposits 24:61–70 (**in Chinese with English abstract**)

He MQ, Liu JJ, Li CY, Li ZM, Liu YP, Yang AP, Sang HQ (2006) 40Ar-39Ar dating of ore quartz from the Baiyangping Cu-Co polymetallic mineralized concentration area, Lanping basin. Chin J Geol 41:688–693 (**in Chinese with English abstract**)

He LQ, Song YC, Chen KX, Hou ZQ, Yu FM, Yang ZS, Wei JQ, Li Z, Liu YC (2009) Thrust-controlled, sediment-hosted, Himalayan Zn–Pb–Cu–Ag deposits in the Lanping foreland fold belt, eastern margin of Tibetan Plateau. Ore Geol Rev 36:106–132

Helal AI, Zahran NF, Rashad AM (2002) Isotope and concentrations of Zn in human blood and serum by ICP-MS. Int J Mass Spectrom 213:217–224

Herrington RJ (2002) Massive sulfide deposits in the South Urals: geological setting within the framework of the Uralide orogen. Mountain Building in the Uralides: Pangaea to the Present. American Geophysical Union, pp 155–182

Hou ZQ, Pan GT, Wang AJ, Mo XX, Tian SH, Sun XM, Ding L, Wang EQ, Gao YF, Xie YL, Zeng PS, Qin KZ, Xu JF, Qu XM, Yang ZM, Yang ZS, Fei HC, Meng XJ, Li ZQ (2006) Metallogenesis in Tibetan collisional orogenic belt: II.Mineralization in late-collisional transformation setting. Mineral Deposits 25:521–543 (**in Chinese with English abstract**)

Hou ZQ, Khin Z, Pan GT, Mo XX, Xu Q, Hu YZ, Li XZ (2007) Sanjiang Tethyan metallogenesis in SW China: Tectonic setting, metallogenic epochs and deposit types. Ore Geol Rev 31:48–87

Hou ZQ, Song YC, Li Z, Wang ZL, Yang ZM, Yang ZS, Liu YC, Tian SH, He LQ, Chen KX, Wang FC, Zhao CX, Xue WW, Lu HF (2008) Trust-controlled, sediments-hosts Pb-Zn-Cu-Ag deposits in eastern and northern margins of Tibetan orogenic belt: geological feature and tectonic model. Mineral Deposits 27:123–143 (**in Chinese with English abstract**)

Jiang SY (2003) Transition metal isotopes: analytical methods and geological applications. Earth Sci Front 10:269–278 (**in Chinese with English abstract**)

Jiang SY, Lu JJ, Gu LX (2001) Determination of Cu, Fe, Zn isotopic compositions by MC-ICPMS and their geological application.

Bull Mineral Petrol Geochem 20:431–433 (**in Chinese with English abstract**)

Jiang S, Woodhead J, Yu J, Pan J, Liao Q, Wu N (2002) A reconnaissance of Cu isotopic compositions of hydrothermal vein-type copper deposit, Jinman, Yunnan, China. Chin Sci Bull 47:247–250

John SG, Rouxel OJ, Craddock PR, Engwall AM, Boyle EA (2008) Zinc stable isotopes in seafloor hydrothermal vent fluids and chimneys. Earth Planet Sci Lett 269:17–28

Johnson CM, Beard BL, Albarede F (2004a) Geochemistry of non-traditional stable isotopes. Rev Mineral Geochem 55:1–21

Johnson CM, Beard BL, Albarède F (2004b) Geochemistry of non-traditional stable isotopes. Rev Mineral Geochem 55:453

Kelley KD, Wilkinson JJ, Chapman JB, Crowther HL, Weiss DJ (2009) Zinc isotopes in sphalerite from base metal deposits in the Red Dog district, Northern Alaska. Econom Geol 104:767–773

Kesler SE, Ruiz J, Jones LM (1983) Strontium isotopic geochemistry of fluorite mineralization (Coahuila, Mexico). Isot Geosci 1:65–75

Kimball BE, Mathur R, Dohnalkova AC, Wall AJ, Rankel RL, Brantley SL (2009) Copper isotopic fractionation in acid mine drainage. Geochim Cosmochim Acta 73:1247–1263

Korte C, Kozur HW, Bruckschen P (2003) Strontium isotope evolution of Late permian and Triassic seawater. Geochim Cosmochim Acta 67:47–62

Lange S, Chaudhuri S, Clauer N (1983) Strontium isotope evidence for the origin of barites and sulfides from the Mississippi Valley-type ore deposits in Southeast Missouri. Econ Geol 78:1255–1261

Larson PB, Maher K, Ramos FC, Chang ZS, Gaspar M, Meinert LD (2003) Copper isotope ratios in magmatic and hydrothermal ore-forming environments. Chem Geol 201:337–350

Li XZ, Liu ZQ, Pan GS (1991) Units partition of tectonic structure and evolution of earth history in southwest Sanjiang region. Acta of Chengdu Geology and Commodity Institute of Chinese Academy of Geosciences (13), Beijing: Geological Publishing House **(in Chinese)**

Li XZ, Liu WJ, Wang YZ, Zhu QW (1999) Tectonic evolution of the tethys and mineralization in the Sanjiang Region. S.W. China. Geological Publishing House, p 258 (**in Chinese**)

Li J, Zhu XK, Tang SH (2008a) Cu isotope fractionation during low temperature processes. Acta Petrol Mineral 27:298–304 (**in Chinese with English abstract**)

Li SZ, Zhu XK, Tang SH, He XX, Cai JJ (2008b) The application of MC-ICP-MS to high precision measurement of Zn isotope ratios. Acta Petrol Mineral 27:273–278 (**in Chinese with English abstract**)

Li ZQ, Yang ZM, Zhu XK, Hou ZQ, Li SZ, Li ZH, Wang Y (2009) Cu isotope composition of Qulong porphyry Cu deposit. Tibet Acta Geol Sinica 83:1985–1996 (**in Chinese with English abstract**)

Li WQ, Jackson SE, Pearson NJ, Graham S (2010) Copper isotopic zonation in the Northparkes porphyry Cu–Au deposit, SE Australia. Geochim Cosmochim Acta 74:4078–4096

Li DD, Liu SA, Li SG (2015) Copper isotope fractionation during adsorption onto Kaolinite: experimental approach and applications. Chem Geol 396:74–82

Liao ZT, Chen YK (2005) Nature and evolution of Lanping-Simao basin prototype. J Tongji Univ (Nat Sci) 33:1528–1531 (**in Chinese with English abstract**)

Liu SA, Teng FZ, Li S, Wei GJ, Ma JL, Li D (2014) Copper and iron isotope fractionation during weathering and pedogenesis: insights from saprolite profiles. Geochim Cosmochim Acta 146:59–75

Liu JJ, Zhai DG, Li ZM, He MQ, Liu YP, Li CY (2010) Occurrence of Ag Co, Bi and Ni elements and its genetic significance in the baiyangping silver-copper polymetallic metallogenic concentration area, Lanping basin, southwestern China. Acta Petrologica Sinica 26:1646–1660 (**in Chinese with English abstract**)

Loss RD, Lu G, G.W. (1990) Zinc isotope anomalies in Allende meteorite inclusions. Astrophys J 360:L59–L62

Lu BX, Qian XG (1999) Petrology research on the deep source inclusions of alkali volcanic rock and alkali-rich porphyry in the Cenozoic Era at western Yunnan. J Yunnan Geol 18:127–143 (**in Chinese with English abstract**)

Lu JJ, Guo WM, Chen WF, Jiang SY, Li J, Yan XW, Xu ZW (2008) A metallogenic model for the Dong guashan Cu–Au deposit of Tongling, Anhui Province. Acta Petrol Sin 24:1857–1864 (**in Chinese with English abstract**)

Luck JM, Othman DB, Barrat JA, Albarède F (2003) Coupled ^{63}Cu and ^{16}O excesses in chondrites. Geochim Cosmochim Acta 67:143–151

Luck JM, Othman DB, Albarède F (2005) Zn and Cu isotopic variations in chondrites and iron meteorites: early solar nebula reservoirs and parent-body processes. Geochim Cosmochim Acta 69:5351–5363

Ludwig K (1982) A computer program to convert raw U–Th–Pb isotope ratios to blank-corrected isotope ratios and concentrations with associated error calculation. OF-88-0557. U.S. Geological Survey

Luo JL, Yang YH, Zhao Z, Chen JT, Yang JZ (1994) Evolution of the Tethys in Western Yunnan and mineralization for main metal deposits. Geological Publishing House, Beijing, pp 1–340 **(in Chinese)**

Maher KC, Larson PB (2007) Variation in copper isotope ratios and controls on fractionation in hypogene skarn mineralization at Coroccohuayco and Tintaya. Peru Econ Geol 102:225–237

Maréchal CN, Albarède F (2002) Ion-exchange fractionation of copper and zinc isotopes. Geochim Cosmochim Acta 66:1499–1509

Maréchal CN, Sheppard SMF (2002) Isotope fractionation of Cu and Zn between chloride and nitrate solutions and malachite or smithsonite at 30 °C and 50 °C. Geochim Cosmochim Acta 66:S484

Maréchal CN, Télouk P, Albarède F (1999) Precise analysis of copper and zinc isotopic compositions by plasma-source mass spectrometry. Chem Geol 156:251–273

Maréchal CN, Nicolas E, Douchet C, Albarède F (2000) Abundance of zinc isotopes as a marine biogeochemical tracer. Geochem Geophys Geosyst 1:1–15

Markl G, Lahaye Y, Schwinn G (2006) Copper isotopes as monitors of redox processes in hydrothermal mineralization. Geochim Cosmochim Acta 70:4215–4228

Mason TFD (2003) High precision transition metal isotope analysis by plasma-source mass spectrometry and implications for low temperature geochemistry. Dr. Sci. thesis, Imperial College, London, 287

Mason TFD, Weiss DJ, Horstwood M, Parrish RR, Russell SS, Mullane E (2004a) High precision Cu and Zn isotope analysis by plasma source mass spectrometry: part 1. Spectral interferences and their correction. J Anal At Spectrom 19:209–217

Mason TFD, Weiss DJ, Horstwood M, Parrish RR, Russell SS, Mullane E (2004b) High precision Cu and Zn isotope analysis by plasma source mass spectrometry: part 2. Correcting for mass bias discrimination effects. J Anal At Spectrom 19:218–226

Mason TFD, Weiss DJ, Chapman JB, Wilkinson JJ, Tessalina SG, Spiro B, Horstwood MSA, Spratt J, Coles BJ (2005) Zn and Cu isotopic variability in the Alexandrinka volcanic-hosted massive sulfide (VHMS) ore deposit, Urals, Russia. Chem Geol 221:170–187

Mathur R, Ruiz J, Titley S, Liermann L, Buss H, Brantley S (2005) Cu isotopic fractionation in the supergene environment with and without bacteria. Geochim Cosmochim Acta 69:5233–5246

Mathur R, Titley S, Barra F, Brantley S, Wilson M, Phillips A, Munizaga F, Maksaev V, Vervoort J, Hart G (2009) Exploration potential of Cu isotope fractionation in porphyry copper deposits. J Geochem Explor 102:1–6

Mathur R, Jin L, Prush V, Paul J, Ebersole C, Fornadel A, Williams J, Brantley S (2012) Cu isotopes and concentrations during weathering of black shale of the Marcellus Formation, Huntingdon County, Pennsylvania (USA). Chem Geol 304:175–184

Moynier F, Albarede F, Herzog G (2006) Isotopic fractionation of Zn, Cu and Fe in lunar materials. Geochim Cosmochim Acta 70:6103–6117

Nakai I, Sugitani Y, Nagashima K (1978) X-ray photoelectron spectroscopic study of copper minerals. J Inorg Nucl Chem 40:781–791

Navarrete JU, Borrok DM, Viveros M, Ellzey JT (2011) Copper isotope fractionation during surface and intracellular incorporation by bacteria. Geochim Cosmochim Acta 75:784–799

Norman DI, Landis GP (1983) Source of mineralizing components in hydrothermal ore fluids: evidence by $^{87}Sr/^{86}Sr$ and stable isotope data from the Pasto Bueno deposit. Peru Econ Geol 78:1375–1378

Norman M, McCulloch M, O'Neill H, Brandon A (2004) Magnesium isotopes in the Earth, Moon, Mars, and Pallasite parent body: high-precision analysis of olivine by laser-ablation multi-collector ICPMS. Lunar Planet. Sci. XXXV. Lunar Planet. Inst., Houston, Abstract, 1447

Pašava J, Tornos F, Chrastný V (2014) Zinc and sulfur isotope variation in sphalerite from carbonate-hosted zinc deposits, Cantabria, Spain. Miner Deposita 49:797–807

Pearce CI, Pattrick RAD, Vaughan DJ, Henderson CMB, van der Laan G (2006) Copper oxidation state in chalcopyrite: mixed Cu d9 and d10 characteristics. Geochim Cosmochim Acta 70:4635–4642

Pekala M, Asael D, Butler IB, Matthews A, Rickard D (2011) Experimental study of Cu isotope fractionation during the reaction ofaqueous Cu(II) with Fe(II) sulphides at temperatures between 40 and 2008C. Chem Geol 289:31–38

Peng JT, Hu RZ, Deng HL (2001) Strontium isotopic geochemistry of Xikuangshan antimony deposit. Geochim 30:248–256 (**in Chinese with English abstract**)

Pichat S, Douchet C, Albarede F (2003) Zinc isotope variations in deep-sea carbonates from the eastern equatorial Pacific over the last 175Ka. Earth Planet Sci Lett 210:167–178

Poitrasson F, Levasseur S, Teutsch N (2005) Significance of iron isotope mineral fractionation in pallasites and iron meteorites for the core-mantle differentiation of terrestrial planets. Earth Planet Sci Lett 234:151–164

Pokrovsky OS, Viers J, Freydier R (2005) Zinc stable isotope fractionation during its adsorption on oxides and hydroxides. J Colloid and Interface Sci 291:192–200

Pokrovsky O, Viers J, Emnova E, Kompantseva E, Freydier R (2008) Copper isotope fractionation during its interaction with soil and aquatic microorganisms and metal oxy (hydr) oxides: possible structural control. Geochim Cosmochim Acta 72:1742–1757

Prokin VA, Buslaev FP, Nasedkin AP (1998) Types of massive sulfide deposits in the Urals. Miner Depos 34:121–126

Qian P, Lu JJ, Liu FX (2006) Isotopic tracing of ore forming source materials in the porphyry copper deposit of Dexing, Jiangxi Province. Glob Geol 25:135–140 (**in Chinese with English abstract**)

Qin GJ, Zhu SQ (1991) Genetic model and prospecting prediction of Jinding Pb–Zn ore deposit. Journal of Yunan Geology 10:145–190 (**in Chinese**)

Rehkämper M, Schönbächler M, Stirling C (2001) Multiple collector ICP-MS: introduction to instrumentation, measurement techniques and analytical capabilities. Geostandard Newsl 25:23–40

Rosman KJR (1972) A survey of the isotopic and elemental abundance of zinc. Geochim Cosmochim Acta 36:801

Rosman KJR, Taylor PDP (1998) Isotopic compositions of the elements 1997. J Anal At Spectrom 13:45–55

Rouxel O, Fouquet Y, Ludden JN (2004) Copper isotope systematics of the Lucky Strike, Rainbow, and Logatchev sea-floor hydrothermal fields on the Mid-Atlantic Ridge. Econ Geol 99:585–600

Savard MM, Chi GX, Sami T, William-Johns AE, Leigh K (2000) Fluid inclusion and carbon, oxygen and strotium isotope study of the Polaris Mississippi Valley-type Zn–Pb deposit, Canadian Arctic Archipelago: implication for ore genesis. Miner Deposita 35:495–510

Scott SD (1981) Small chimneys from Japanese Kuroko deposits. In: Goldie R, Botrill TJ (eds) Seminars on seafloor hydrothermal systems. Geoscience Canada, pp 103–104

Shanks W, Seyfried W (1987) Stable isotope studies of vent fluids and chimney minerals, southern Juan de Fuga Ridge: sodium metasomatism and seawater sulphate reduction. J Geophys Res 92:11387–11399

Shao ZG, Meng XG, Feng XY, Zhu DG (2003) Tectonic characteristics of the Baiyangping-Huachangshan ore belt, Yunnan Province and its orecontrolling effect. J Geomech 9(3):246–253 (**in Chinese with English abstract**)

Shields WR, Goldich SS, Garner EL, Murphy TJ (1965) Natural variations in the abundance ratio and the atomic weight of copper. J Geophys Res 70:479–491

Simonetti A, Buzon MR, Creaser RA (2008) In situ elemental and Sr isotope investigation of human tooth enamel by Laser Ablation-(MC)-ICP-Ms: successes and pitfalls. Archaeometry 50:371–385

Sigov A (1969) Mesozoic and Cenozoic ore formation in the Urals. Nedra, Moscow

Strelow FWE (1978) Distribution coefficients and anion exchange behaviour of some elements in hydrobromic-nitric acid mixtures. Anal Chem 50:1359–1361

Tang YY (2013) Abnormal enrichment mechanisms of ore-forming metals in the Jinding Zn–Pb Deposit, Yunnan Province, China. Dr. Sci. Thesis, The University of Chinese Academy of Science, pp 1–129 **(in Chinese with English abstract)**

Tang SH, Zhu XK, Cai JJ, Li SZ, He XX, Wang JH (2006a) Chromatographic separation of Cu, Fe and Zn using AG M P-1 anion exchange resin for isotope determination by MC-ICPMS. Rock Miner Anal 25:5–8 (**in Chinese with English abstract**)

Tang SH, Zhu XK (2006b) Separation of some elements using AGMP-1 Anion Exchange Resin. Geol J China Univ 12(3):398–403 (**in Chinese with English abstract**)

Tessalina SG, Maslennikov VV, Zaykov VV, Orgeval JJ (1999) Ore facies of the Alexandrinka massive sulphide deposit, South Urals. In: Stanley C, (ed) Mineral deposits: processes to processing. Balkema, pp 601–604

Tessalina SG, Zaykov VV, Orgeval JJ, Auge T, Omeneto B (2001) Mafic-ultramafic hosted massive sulphide deposits in southern Urals (Russia). Mineral deposits at the beginning of the 21st century. Balkema, Rotterdam, pp 353–356

Tian HL (1997) The geological features of Baiyangping Cu-Ag polymetallic deposit, Lanping. Yunnan Geol 16:105–108 (**in Chinese with English abstract**)

Tian HL (1998) The geological features of Sanshan polymetallic deposit. Lanping. Yunnan Geol 17(2):199–206 (**in Chinese with English abstract**)

The Third Geological Survey Institute of Yunnan Geological Survey (2003) Geological evaluation report of Baiyangping copper

silver lead zinc cobalt mineralization concentration area, Lanping, Yunnan, pp 1–266 **(in Chinese with English abstract)**

Vance D, Archer C, Bermin J, Kennaway G, Cox EJ, Statham PJ, Lohan MC, Ellwood MJ (2006) Zn isotopes as a new tracer of metal micronutrient usage in the oceans. Geochimica et Cosmochimica Acta 70:A666

Viezer J (1989) Strotium isotope in seawater through time. Annu Rev Earth Planet Sci 17:141–167

Walker EC, Cuttitta F, Senftle FE (1958) Some natural variations in the relative abundances of copper isotopes. Geochim Cosmochim Acta 15:183–194

Wang E, Burchfiel BC (1997) Interpretation of Cenozoic tectonics in the right-lateral accommodation zone between the Ailao Shan shear zone and the eastern Himalayan syntaxis. Int Geol Rev 39:191–219

Wang F, He MY (2003) Lead and sulfur isotopic tracing of the ore-forming material from the Baiyangping copper-silver polymetallic deposit in Lanping, Yunnan. Sediment Geol Tethyan Geol 23(2):82–85 (**in Chinese with English abstract**)

Wang Y, Zhu XK (2010) Application of Zinc isotopes to study mineral deposit: a review. Miner Deposit 29:843–852 (**in Chinese with English abstract**)

Wang JH, Yin A, Harrison TM, Grove M, Zhang YQ, Xie GH (2001) A tectonic model for Cenozoic igneous activities in the eastern Indo-Asian collision zone. Earth Planet Sci Lett 188:123–133

Wang YB, Zeng PS, Li YH, Tian SH (2004) He–Ar isotope composition of Jinding and Baiyangping mineral deposit and its significance. J Mineral Petrol 24(4):76–80 **(in Chinese with English abstract)**

Wang XH, Song YC, Hou ZQ, Zhang HR, Liu YC, Yang ZS, Yang TN, Pan XF, Wang SX, Xue CD (2011) Characteristics of trace elements and S-Pb isotopes in sphalerites from lead-zinc polymetallic deposits in Fulongchang area, Lanping basin, western Yunnan Province, and their implications. Acta Petrologica Et Mineralogica 30:45–59 (**in Chinese with English abstract**)

Weiss DJ, Mason TFD, Zhao FJ, Kirk GJD, Coles BJ, Horstwood MSA (2005) Isotopic discrimination of Zn in higher plants. New Phytol 165:703–710

Weyer S, Anbar AD, Brey GP, MüInker C, Mezger K, Woodland AB (2005) Iron isotope fractionation during planetary differentiation. Earth Planet Sci Lett 240:251–264

Wilkinson JJ, Weiss DJ, Mason TFD, Coles BJ (2005) Zinc isotope variation in hydrothermal systems: preliminary evidence from the Irish midland ore fields. Econ Geol 100:583–590

Xu QD, Li JW (2003) Migration of ore-forming fluids and its relation to zoning of mineralization in northern Lanping Cu-polymetallic area, Yunnan Province: evidence from fluid inclusions and stable isotopes. Miner Deposit 22:366–376 (**in Chinese with English abstract**)

Xue CJ, Wang DH, Chen YC, Yang JM, Yang WG (2000a) Helium, Argon, and Xenom isotopic compositions of ore-forming fluids in Jingding-Baiyangpin plymetallic deposits, Yunnan, Southwest China. Acta Geologica Sinca 74:521–528

Xue CJ, Yang JM, Chen YC (2000b) Ore-forming characteristics of Baiyangping Cu–Co deposit, Lanping. In: Cheng YC (ed) A research on the endogenetic mineralization of Himalayan Era. Seismological Publishing House, Beijing, pp 69–83 (**in Chinese**)

Xue CJ, Chen YC, Wang DH, Yang JM, Yang WG, Yang QB (2002) Analysis of ore-forming background and tectonic system of Lanping basin, western Yunnan Province. Mineral Deposits 21:36–44 (**in Chinese with English abstract**)

Xue CJ, Chen YC, Yang JM, Wang DH, Yang WG, Zeng R (2003) Geology and isotopic composition of helium, neon, xenon and metallogenic age of the Jinding and Baiyangping ore deposits, northwest Yunnan, China. Sci China (Ser D) 33:315–322 (**in Chinese**)

Xue CJ, Zeng R, Gao YB, Zhu HP, Zhao SH, Li YQ (2006) Fluid Processes of a heavy metallogenesis at Jin ding, Lan Ping, SW-China. Acta Petrologica Sinica 22:1031–1039 (**in Chinese with English abstract**)

Xue CJ, Zeng R, Liu SW, Chi GX, Qing HR, Chen YC, Yang JM, Wang DH (2007) A review of the geologic, fluid inclusion and isotopic characteristics of the Jinding Zn-Pb Deposit, western Yunnan, China. Ore Geol Rev 31:337–359

Yang WG, Yu XH, Li WC, Dong FL, Mo XX (2003) The characteristics of metallogenic fluids and metallogenic mechanism in Baiyangping silver and polymetallic mineralization concentration area in Yunnan Province. Geoscience 17:27–33 (**in Chinese with English abstract**)

Yin HH, Fang WM, Lin G (1990) Deep factors on the Lanping-Simao basin evolution and mantle-crust complex mineralizations. Geotectonic et Metallogenia 4(2):113–124 (**in Chinese with English abstract**)

Zhang EX (2005) On the genesis of ore deposits in west metallogetic zone of Baiyangping Cu-Ag polymetallic deposit concentration area, Lanping. Yunnan Geol 24:282–289 (**in Chinese with English abstract**)

Zhao HB (2006) Study on the characteristics and metallogenic condition of copper[1]polymetallic deposits in middle-northern Lanping Basin, Western Yunnan. Published PhD. Dissertation, China University of Geosciences, p 123 (**in Chinese with English abstract**)

Zhong DL, Ding L (1993) To discuss Gondawana continent, Asian Continent Hyperplasia and Asian Hyperplasia from Tethys evolution in Sanjiang and its neighbor. Seismological Press, Beijing, pp 5–8 **(in Chinese)**

Zhou JX, Huang ZL, Zhou MF, Zhu XK, Philippe M (2014) Zinc, sulfur and lead isotopic variations in carbonate-hosted Pb–Zn sulfide deposits, southwest China. Orel Geol Rev 58:41–54

Zhu XK, O'Nions RK, Guo Y, Belshaw NS, Rickard D (2000) Determination of natural Cu-isotope variation by plasma source mass spectrometry: implications for use as geochemical tracers. Chem Geol 163:139–149

Zhu XK, Guo Y, O'Nions RK, Young ED, Ash RD (2001) Iron isotope homogeneity in the early Solar Nebula. Nature 412:311–313

Zhu XK, Guo Y, Williams RJP, O'Nions RK, Matthews A, Belshaw NS (2002) Mass fractionation processes of transition metal isotopes. Earth Planet Sci Lett 200:47–62